Universidade de Aveiro Departamento de Engenharia Mecânica

2019

JOÃO LIMA OLIVEIRA

ESTUDO DE MELHORIA DE UMA LIGA DE ALUMÍNIO UTILIZADA NA INDÚSTRIA AERONÁUTICA

STUDY OF IMPROVEMENT OF AN ALUMINIUM ALLOY USED IN THE AERONAUTICAL INDUSTRY

Universidade de Aveiro Departamento de Engenharia Mecânica

2019

JOÃO LIMA OLIVEIRA

ESTUDO DE MELHORIA DE UMA LIGA DE ALUMÍNIO UTILIZADA NA INDÚSTRIA AERONÁUTICA

STUDY OF IMPROVEMENT OF AN ALUMINIUM ALLOY USED IN THE AERONAUTICAL INDUSTRY

Dissertação apresentada à Universidade de Aveiro para cumprimento dos requisitos necessários à obtenção do grau de Mestre em Engenharia Mecânica, realizada sob a orientação científica da Doutora Gabriela Tamara Vincze, Investigadora Auxiliar do Departamento de Engenharia Mecânica da Universidade de Aveiro

Esta dissertação teve o apoio dos projetos:

- POCI-01-0145-FEDER-032362 - Programa Operacional Competitividade e Internacionalização, na sua componente FEDER, e da Fundação para a Ciência e a Tecnologia, I.P./MCTES, na sua componente de Orçamento de Estado;
- UID/EMS/00481/2019-FCT - FCT - Fundação para a Ciência e a Tecnologia;
- CENTRO-01-0145-FEDER-022083 - Programa Operacional Regional do Centro (Centro2020), através do Portugal 2020 e do Fundo Europeu de Desenvolvimento Regional.

o júri

presidente

Prof. Doutor João Paulo Davim Tavares da Silva
Professor Associado C/Agregação da Universidade de Aveiro

Prof. Doutor Fábio Jorge Pereira Simões
Professor Adjunto do Instituto Politécnico de Leiria

Doutora Gabriela Tamara Vincze
Investigadora Auxiliar da Universidade de Aveiro

agradecimentos

Em primeiro lugar deixar um agradecimento à Doutora Gabriela Vincze pelo acompanhamento e disponibilidade durante este longo e atribulado período. É também reconhecido o esforço prestado pelo Prof. Augusto Lopes e pelo Eng. Tiago Silva do Departamento de Microscopia da UA.

O maior agradecimento vai para a minha família. Em especial para a minha irmã, mãe e pai que me deram a oportunidade e a motivação para me formar na área que gosto. A este agradecimento junto uma promessa de retribuição por todo o suporte durante cinco anos.

Um obrigado ao Luís Quental e à Sara Castro por mostrarem sempre disponibilidade para me ajudarem. O meu mérito será sempre também deles.

Finalmente, a todos os colegas que tornaram Aveiro a minha segunda casa, um muito obrigado. Ficam na memória as noitadas a estudar, os cafés até tarde e muitas mais aventuras.

palavras-chave

aeronáutica, liga de alumínio, laminagem assimétrica, comportamento mecânico, textura cristalográfica

resumo

A indústria aeronáutica aposta cada vez mais no desenvolvimento de novos materiais que respondam às exigências de performance características desta área. Estes desenvolvimentos estão associados a uma procura por soluções mais económicas.

Este trabalho estuda a possibilidade de melhoramento da liga de alumínio AA6061 através dos processos de laminagem assimétrica e tratamentos térmicos.

É explorado o efeito dos vários tipos de laminagem (convencional e assimétrica), assim como doutros parâmetros deste processo. Amostras previamente recristalizadas são submetidas a laminagem com diferentes razões entre as velocidades dos rolos (1, 3 e 1,36), taxas de redução (20% e 50%) e rotas de deformação (convencional, assimétrica contínua e assimétrica reversa).

As propriedades mecânicas e textura cristalográfica das amostras foram analisadas de forma a relacionar os resultados obtidos com as diferentes condições do processo. A obtenção de dados foi feita através de testes de dureza e tração e de análise EBSD.

Depois da laminagem e recozimento obtiveram-se aumentos significativos na dureza das amostras. Todas as amostras apresentam grandes aumentos nos valores das tensões de cedência e de rotura em detrimento da formalidade, sendo estes efeitos mais acentuado para as amostras processadas com uma taxa de redução de 50%.

A análise de EBSD revela a formação de componentes de textura de cobre {112}<111> e de corte {111}⟨112⟩ e {001}⟨110⟩, que contribuem ao aumento da resistência mecânica.

Conclui-se que é possível melhorar as propriedades mecânicas desta liga de alumínio, registando valores de resistência superiores à liga AA6061-T6.

As limitações referentes à formabilidade do material podem ser revistas com a aplicação de novos tratamentos térmicos em trabalhos futuros.

keywords

aeronautics, aluminium alloy, asymmetric rolling, mechanical response, crystallographic texture

abstract

The aeronautics industry is increasingly investing in the development of new materials that meet the high-performance requirements of this area. These developments are associated with a pursuit for more economical solutions.
This work studies the possibility of improvement of the AA6061 aluminium alloy through asymmetric rolling processes and heat treatments.
The effect of the various types of rolling (conventional and asymmetric), as well as other parameters of this process, is explored. Previously recrystallized samples are subjected to different ratios of the roll's velocities (1, 3 and 1.36), thickness reduction per pass (20% and 50%) and forming routes (conventional, asymmetric continuous and asymmetric reverse).
The mechanical properties and crystallographic texture of the samples were analysed in order to correlate the results obtained with the different process conditions. Data were obtained through hardness and uniaxial tensile tests, and EBSD analysis.
After rolling and annealing, significant increases in hardness were observed in the samples. All samples show a large increase of yield and ultimate tensile stress, while the formability drastically decreases, being more pronounced for sample processed with a 50% rate reduction of thickness.
The EBSD analysis reveals a formation of copper {112} <111>, shear 1 {001}⟨110⟩ and shear 2 {111}⟨112⟩ texture components which contribute to the increase of mechanical strength.
It is concluded that the mechanical properties of this aluminium alloy can be enhanced originating strength values higher than the AA6061-T6 alloy.
The limitations regarding the reduced material formability can be reviewed in the future by applying new heat treatments.

Index

List of Figures

List of Tables

Symbols and Abbreviations

AA- Aluminium alloy;
AHT- Annealing heat treatment;
AS- Annealed samples;
ASR- Asymmetrical rolling;
ASRC- Asymmetrical rolling continuous;
ASRR- Asymmetrical rolling reverse;
ASTM- American Society for Testing and Materials;
BCC- Body-centred cubic;
CNC- Computer numerical control;
CR- Conventional rolling;
EBSD- Electron backscattered diffraction;
FCC- Face -centred cubic;
HCP- Hexagonal closest packed;
HV- Vickers hardness;
NAS- Non annealed samples;
ND- Normal direction;
ODF- Orientation distribution function;
PF- Pole figure;
RD- Rolling direction;
rpp- Thickness reduction per pass;
RT- Recrystallization temperature;
SHT- Solution / Solubilisation heat treatment;
SEM- Scanning electron microscope;
TD- Transverse direction.

1. Introduction

1.1. Motivation

The aeronautical industry is the dream ground for most engineers, and this dissertation responds to the increasing necessity of supplying it with high quality materials at lower costs.
The biggest motivation behind this work is to study the possibility of developing a new material that may impact the aerospace and aeronautical fields.
The future of these industries matches the objectives proposed in this work, which opens a unique opportunity to explore, learn and enrich the technical knowledge in this area. History shows that aluminium is one of the pillars of aerospace and aeronautical developments. Space exploration, including space tourism, is on the brink of a revolution, with the big players starting to fund new researches for solutions that make it affordable.
Being one of the few 100% recyclable materials, aluminium offers a solution of present and future that does not compromise the environment.

1.2. Main objectives

New materials are highly sought in the previously mentioned industries. In the context of making aerospace a more profitable and accessible means, new materials need to be developed to meet the highly demanding technical requirements while offering a low-cost solution.
The idea behind this thesis is to improve the properties of a common aluminium alloy (AA6061) that can be compared with the properties of the aluminium alloys used in the aerospace industry.
The processes used to improve it are rolling combined with heat treatment, both simple and cheap processes that may or may not origin an improvement in the properties of this aluminium alloy.
It is studied the effects of a variety of rolling sequences in the mechanical properties of the samples.
It is expected to see a comparison of the mechanical properties of the samples after rolling, and the differences registered among all the rolling sequences. Data crossing between the mechanical properties and texture information should characterize even further the behaviour of the aluminium alloy when subjected to the referred processes.

(Page intentionally left blank)

2. Literature Review

This chapter introduces some concepts deemed essential to comprehend the concepts and the whole investigation made in this master's thesis.

2.1. Aluminium

There are all kinds of aluminium alloys that can be classified into different numbers according to its chemical composition and properties. Additional letters / numbers might be used to specify the temper as for example 'F' for fabricated, 'O' for annealed, 'H' for strain hardened and 'T' for thermal treatment. The aluminium subdivides into Wrought Aluminium and Cast Aluminium and the numbering system also differs a bit. Tables containing the information about the numbering system are stated below (tables 1 and 2).

Each series of aluminium alloys, alongside their respective composition, forms unique properties providing a wide range of alloys solutions to satisfy the demand of different markets and applications:

- 1xxx series - The purity of the aluminium is about 99%. They are most used for electronical applications and packaging, since they have high thermal and electrical conductivity as well as high deformability and corrosion resistance.
- 2xxx series - Can be enhanced by heat treatments. Have great strength but not great corrosion resistance.
- 3xxx series - With the main component of the alloy being Manganese (except aluminium), it has high formability and moderate strength, allowing it to be used in the production of beverage cans.
- 4xxx series - Used mainly as welding wires, the silicon added into the alloy reduces the melting point of the aluminium.
- 5xxx series - Its high corrosion resistance is ideal for shipbuilding. It has moderate strength and good weldability. Magnesium is the alloying agent.
- 6xxx series - High deformability and capacity of enhancing its strength with heat treatments. Weldable and have great corrosion resistance. Contains Silicon and Magnesium.
- 7xxx series - Very high strength alloy that is heat treatable. Commonly used in the aircraft industry. Zinc and Magnesium are part of the alloy.

Table 1: Wrought aluminium alloys (AMAG Rolling GmbH, 2012).

1xxx	Pure Aluminum
2xxx	Copper
3xxx	Manganese
4xxx	Silicon
5xxx	Magnesium
6xxx	Magnesium and Silicon
7xxx	Zinc
8xxx	Other

Table 2: Cast aluminium alloys (AMAG Rolling GmbH, 2012).

1xx.x	Pure Aluminum
2xx.x	Copper
3xx.x	Silicon and/or Copper and/or Magnesium
4xx.x	Silicon
5xx.x	Magnesium
6xx.x	Not used
7xx.x	Zinc
8xx.x	Tin
9xx.x	Other

As mentioned, many temper designations for different aluminium alloys exist, and some of them are presented below:

- O- annealed, recrystallized. For wrought aluminium only.
- T4- solution heat treated and naturally aged until stabilization.
- T6- solution heat-treated and artificially aged.
- T8- solution heat-treated, cold-worked, and then artificially aged.

The aluminium alloy used in this investigation is the AA6061-T6.

2.1.1. AA6061

The 6061 is a precipitation hardenable Al-Mg-Si alloy that belongs to the 6xxx series.
6xxx alloys are one of the most versatile group of alloys. Their composition, besides aluminium, contains a significant quantity of Magnesium and Silicon which provides the alloy unique mechanical properties that makes this series one of the most versatile.
Its heat-treatable ability allows the improvement of its mechanical properties by heating and cooling, respectively. Its high formability, relatively high strength and optimum corrosion resistance elevate the AA6061 to a status of one of the most practical aluminium alloys. In addition, good

weldability properties are another advantage of AA6061. It is very common to see extruded products from AA6061. Moreover, only one other alloy (AA6063) is more popular.

2.1.2. Aerospace Aluminium alloys

Aluminium alloys play a fundamental role in structural building of aerospace applications. The necessity of specific mechanical properties propels the growth of R&D departments, leading to a perfect symbiosis that provides the creation of new alloys that branch off to other markets.
Aluminium is used in aircrafts since 1930. Different alloys compose different sections of an aircraft. Below, a list of some of the most used materials is stated:

- AA 2014 – Used in landing gears and hydraulic cylinders;
- AA 2219 – Was used to build the external tank for the space shuttle;
- AA 7475 – Frequently applied in wing spars, wing skins and fuselage bulkheads;
- AA 7178 – Aircraft skins are made with this alloy.

Due to their impressive toughness, the 2xxx and 7xxx groups of aluminium alloys contribute the most to aircraft components through the times (figure 1).

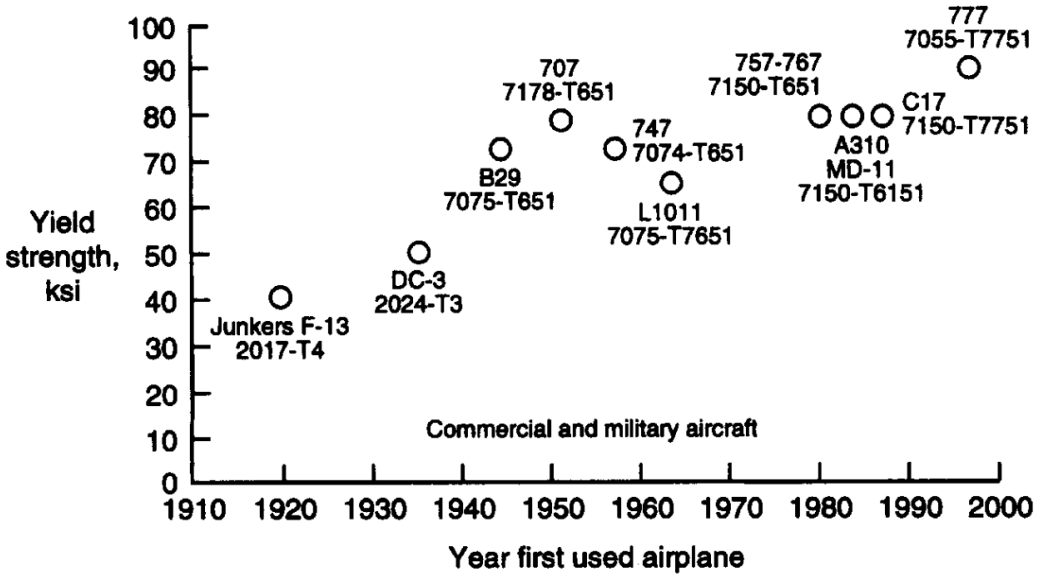

Figure 1: Yield strength of different aluminium alloys and the time they were firstly used (Starke & Staley, 1996).

When designing aircrafts, the knowledge of the requirements of each component is essential to maintain its stability and structural solidity. That way, different aluminium alloys and other materials are used in order to satisfy those same needs (figure 2 and 3).

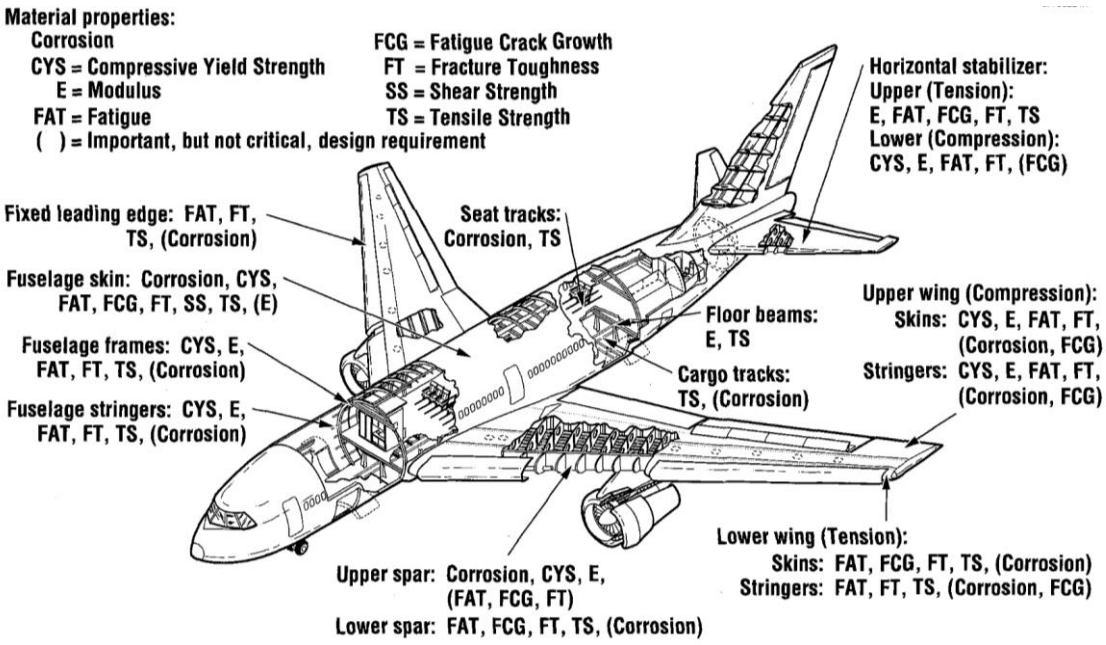

Figure 2: Requirements of the material's properties for each component of a jetliner (Staley & Lege, 1993).

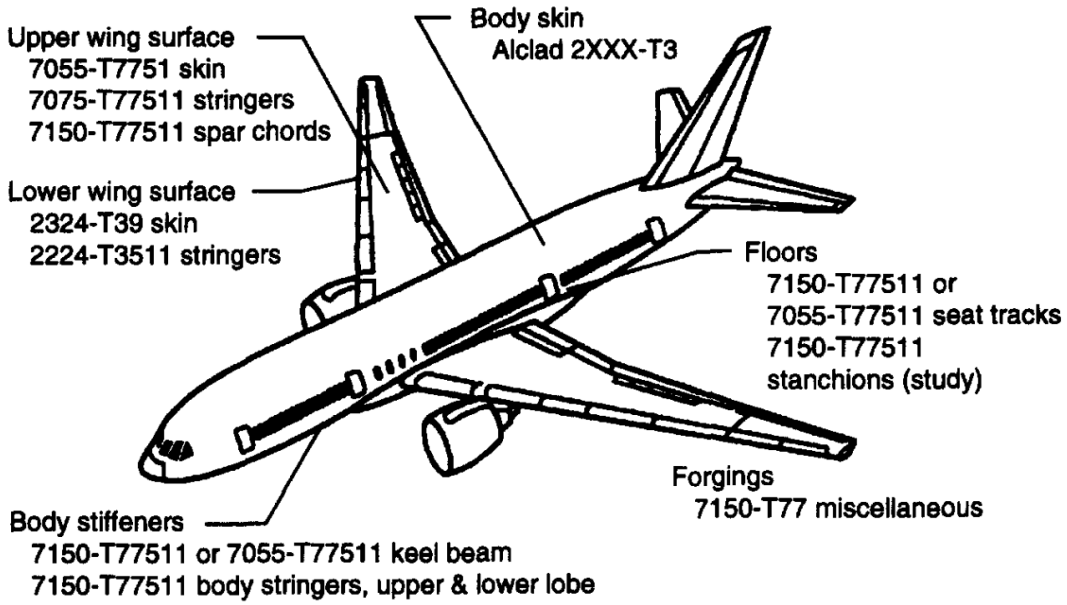

Figure 3: Aluminium alloys used on the Boeing 777 (Starke & Staley, 1996).

Each day new materials emerge suppressing the previous ones, whether being aluminium alloys or even new composite materials. Hence, the enhancement of any of these materials is always welcomed and may, potentially, represent millions in savings for the industry.

An article of Amag et al., 2012 presents the results of different studies for the improvement of the mechanical properties of AA6061 to be used for aerospace applications. In this study, a pre-aging treatment was developed and studied leading to improvements in the strength compared to the

traditional AA6061-T6. The comparison of the pre-aged aluminium 6061-T6* with a 2xxx series aluminium shows the potential of enhancing this material (figure 4).

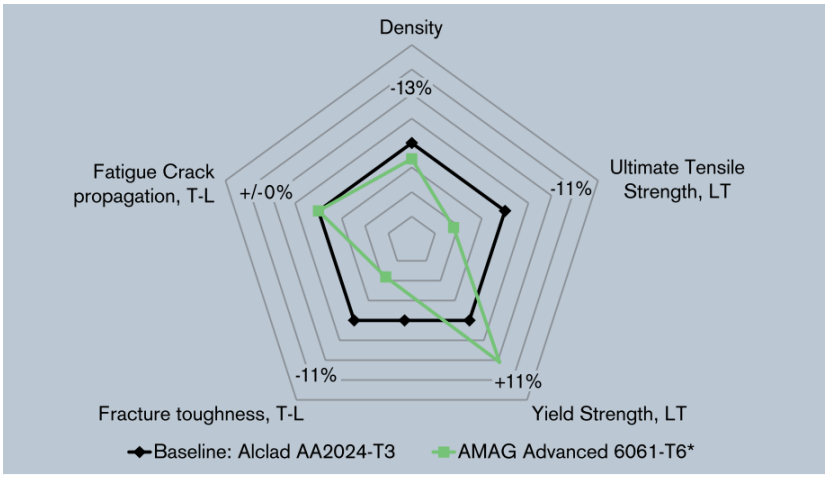

Figure 4: Comparison between 6061-T6 and a 2xxx series aluminium* (AMAG Rolling GmbH, 2012).

The possibilities of creating stronger alloys are not confined to new combinations of heat treating and aging. Strain hardening is one of the most promising processes that lead to improvement. AA6061 allows a wide variety of potential works, being one of the most versatile alloys at the moment.

2.2. Mechanical Properties

2.2.1. Tensile Testing

The stress-strain behaviour of a material registers the deformation when loads are applied into it. There are two types of deformation evidenced in the stress-strain curves, elastic and plastic deformation. The first registers a proportion between the stress and the strain (Young's Modulus), and the phenomenon is named Hooke's Law.

$$\sigma = E * \varepsilon$$

On one hand, the elastic behaviour of the material allows it to return to its original shape without permanent deformation.

On the other hand, the plastic behaviour of the material occurs when the stress applied surpasses the yield strength of the material, resulting in permanent deformation. The yield strength of a material is obtained offsetting the elastic curve by 0.2% of strain.

After yielding, the stress needed to continue the deformation increases till a maximum value, called tensile strength. Afterwards, the material continues to strain, requiring less and less stress to deform it, until reaching its breaking point. It happens due to the decreasing of the cross-section area on which stress is applied.

True Stress-True Strain curves are an alternative way to represent the behaviour of material.

While engineering stress (σ) is the result of the load applied divided by the initial cross-section area, true stress (σ_T) is calculated with the instantaneous values of the cross-section area.
The equipment used in the tensile tests, commonly registers the engineering curve. For that reason, a conversion method is used to obtain the true stress and true strain (ε_T) values.

$$\sigma_T = \sigma(1 + \varepsilon)$$

$$\varepsilon_T = ln(1 + \varepsilon)$$

The visual representation of the curves slightly changes, with the true curve continuing to register an increase in its true stress after the tensile strength point (figure 5).

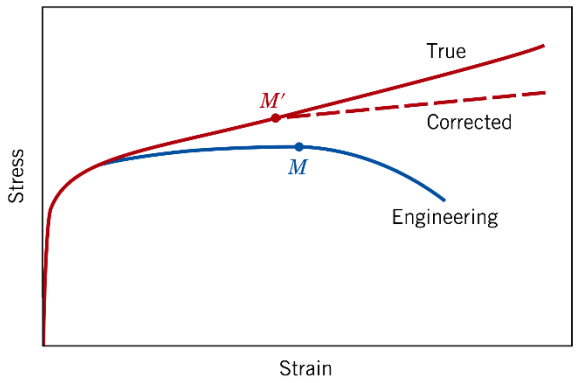

Figure 5: Comparison of the engineering and stress curves (D. Callister Jr. & G. Rethwisch, 2011).

2.2.2. Hardness Testing

The hardness of a material is a property that evaluates its comportment to concentrated plastic deformations. Hardness tests are conducted by indenting a punch into the surface of the tested sample. The characteristics of the shape printed on the sample result on a quantitative evaluation of the material's hardness.
The diffusion of this method happened since it is a quick, inexpensive and non-destructive alternative of the conventional tensile tests, by estimating the values of tensile strength.
There are different methods of hardness testing, Rockwell, Vickers, Brinell, and so on. In this work, hardness values of the samples are done through Vickers Hardness.
Vickers microhardness is measured with a diamond pyramid resulting in a diamond shape print in the sample (figure 6).

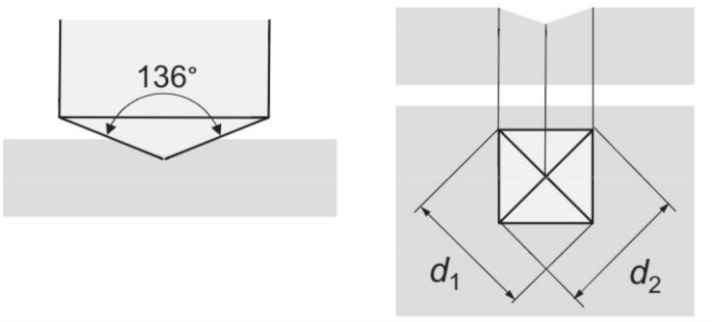

Figure 6: Vickers Hardness a) Punch and b) indentation (Koch, Bierögel, & Seidler, 2014).

The values are calculated by extracting the d_1 and d_2 dimensions of the indentation, result of the applied load (P).

$$HV = (1.854 * P)/(d_1 * d_2)$$

2.3. Microstructure

When the atoms in a solid material are arranged in patterns over large atomic distances it is labelled as a crystalline material. The way the atoms distribute themselves under solidification defines the type of crystalline structure that confer the material some of its properties.

2.3.1. Crystalline Structure

All metals (and many ceramics and polymers) are crystalline materials. The relation of atoms with each other in the lattice is commonly represented by an atomic hard-sphere model. Almost every kind of metals present FCC, BCC or HCP lattice. Aluminium, for example, has an FCC crystalline structure (figure 7).

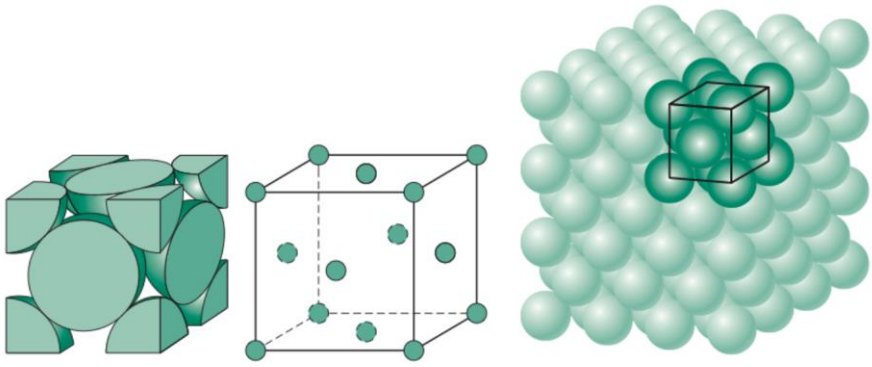

Figure 7: Representation of an FCC crystalline structure, a) hard-sphere model, b) reduced-sphere unit cell, and c) a cluster of atoms, (Wulff et al., 1967)*, (adapted).*

FCC is a cubic central system. The crystallographic directions are represented in the unit cell dimensions with [u,v,w] notation (figure 8).

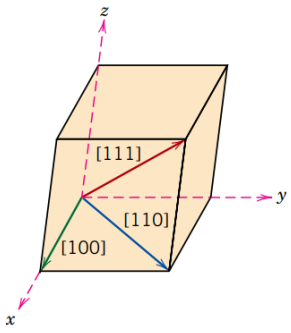

Figure 8: Crystallographic directions of cubic crystals (D. Callister Jr. & G. Rethwisch, 2011).

The crystallographic planes are specified by Miler indices (hkl). The indices represent the intersection of the plane by the reciprocal multiples of the (x,y,z) axis (figure 9).

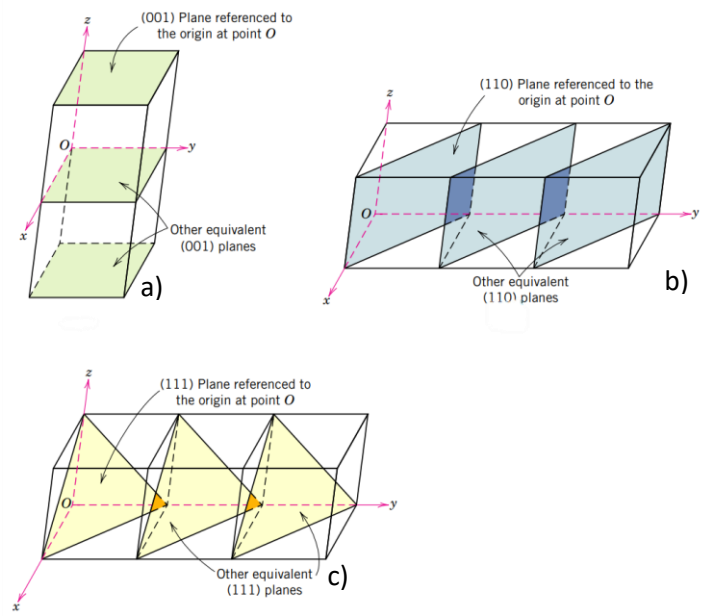

Figure 9: Crystallographic planes, a) (001), b) (110), and c) (111), (D. Callister Jr. & G. Rethwisch, 2011)*, (adapted).*

Polycrystal materials have a plural number of grains with distinct orientations from each one of them. It is essential to relate the orientation of the grains to the used macroscopic references. The notation used to define the orientation is through a plane {hkl}, parallel to the normal direction ND and a direction <uvw> parallel to the rolling direction RD.
Another, and more meticulous, representation of the grains' orientation presented in figure 10, is through 3 angles, named Euler angles (φ_1, ϕ, φ_2).

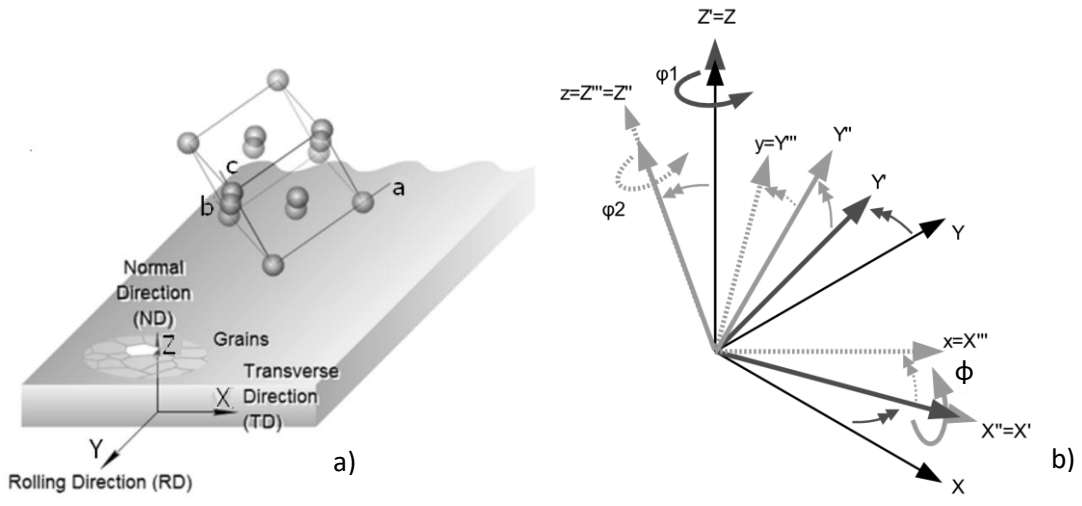

Figure 10: Representation of a) ND and TD direction and b) Euler angles, (Simões, 2008)*, (adapted).*

The texture of a sample is characterized by the size and shape of the grains. Special equipment like goniometer or scanning electron microscope equipped with EBSD system are required to obtain a detailed analysis of the texture.

2.3.2. EBSD and Texture

EBDS (Electron Backscattered Diffraction) is a technique of characterization of the materials' surface. With it, it is possible to identify the crystalline phases, the orientation of the lattice and to define the texture of the material.
It is a technique implemented in SEM (Scanning Electron Microscope) that correlate Kikuchi bands generated from individual grains of material to their crystal structure and their orientation. This information allows us to obtain the poles figures and ODFs (Orientation Distribution Function) and thus determine the texture components existed in the samples. Pole figures are a stereographic projection of the crystallographic directions presented in the grains. The distribution of the density is embodied through an agglomerate of points or through colour contour levels (figure 11).

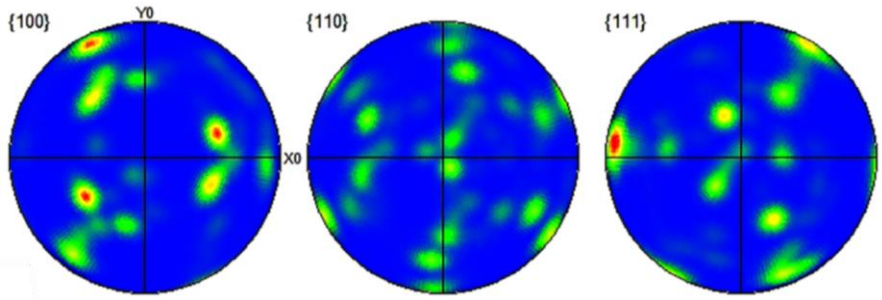

Figure 11: Pole figures of an aluminium alloy (Azimi-Roeen et al., 2018).

Other representation method of the texture are the ODFs. To simplify the representation of the 3D space created by Euler Angles, the density of the grain orientation is represented by several sections of the φ_2 angle (image 12).

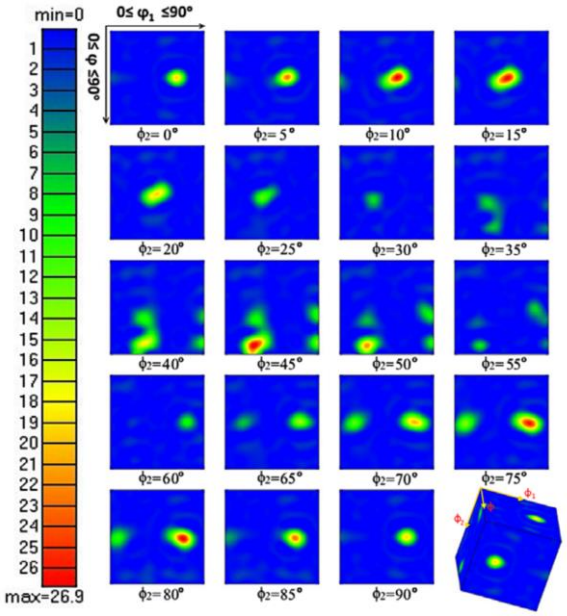

Figure 12: ODFs of an aluminium alloy (Azimi-Roeen et al., 2018).

FCC materials have a set of ideal components of texture (table 3), whether they are deformation or recrystallization components.

Table 3: Texture components of FCC materials, (Simões, 2008).

Type	Component	{hkl}<uvw>	Euler Angles (Bunge)		
			φ1	θ	φ2
Deformation	Bs (brass)	{011}<211>	35	45	0
	S	{123}<634>	55	35	65
	Cu (copper)	{112}<111>	90	30	45
	Shear1	{001}<110>	0	0	45
	Shear2	{111}<112>	90	55	45
	Shear3	{111}<110>	0	55	45
	Shear4	{112}<110>	0	35	45
Recrystallization	Goss	{011}<001>	0	45	0
	Cube	{001}<100>	0	0	0
	RCRD1	{013}<100>	0	20	0
	RCRD2	{023}<100>	0	35	0
	RCND1	{001}<310>	20	0	0
	RCND2	{001}<320>	35	0	0
	P	{011}<122>	70	45	0
	Q	{013}<231>	55	20	0
	R	{124}<211>	55	75	25

The ideal texture components for ODF's sections φ_2=0°, φ_2=45°and φ_2=65° are represented in figure 13.

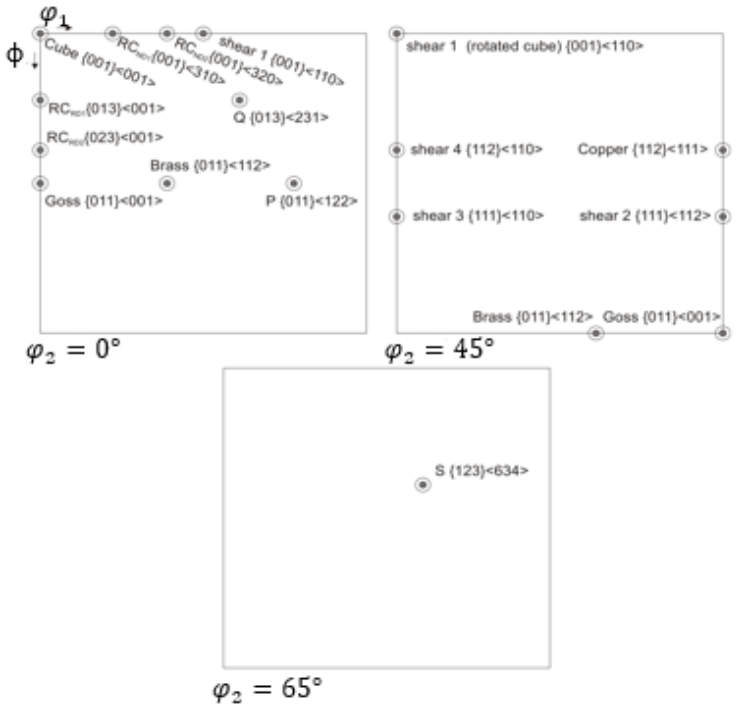

Figure 13: Localization of the texture's components on 3 ODFs sections, *(Simões, 2008)*, (adapted).

Other authors refer other legends of texture components for aluminium. Each representation serves as a key (figure 14) to interpret the EBSD analysis in following steps.

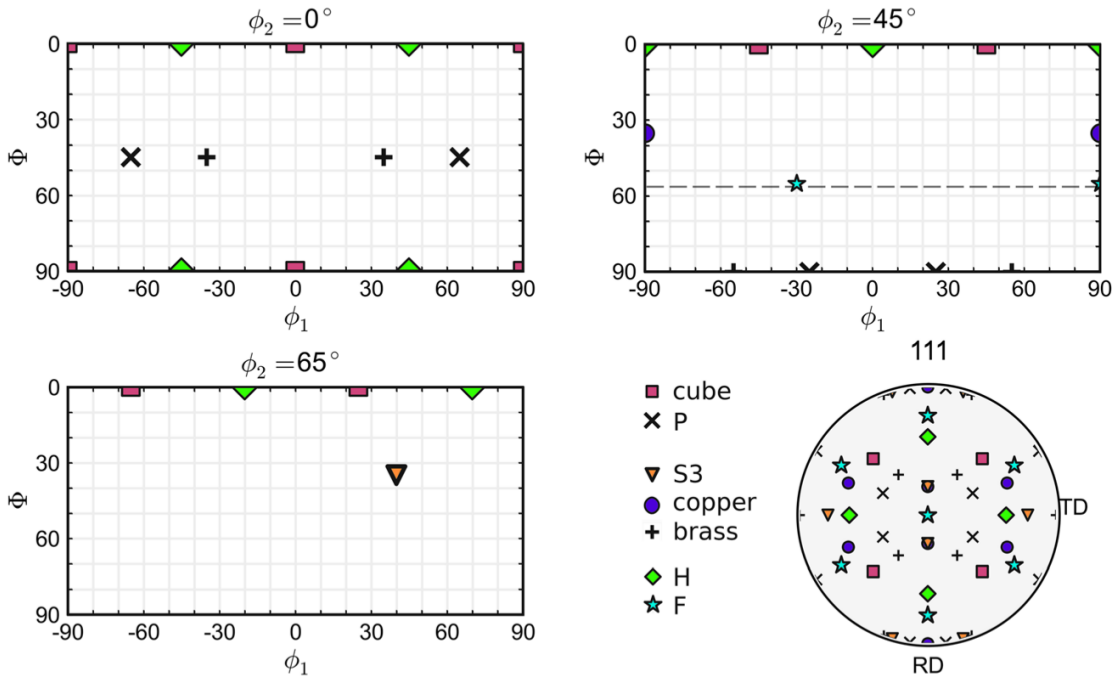

Figure 14: ODFs and PFs legends (Shore et al 2018).

2.4. Deformation

Mechanical deformation occurs when loads are applied to the material, forcing it to change shape or size. The plastic deformation, unlike the elastic deformation, is not reversible, and it happens when the stresses employed reach the Yield Stress of the material.

There are two mechanism of plastic deformation in metals: slip and twinning. Slip (figure 15) is the leading mechanism of deformation in metals and is the one acting in aluminium alloys. A permanent displacement of crystal blocks moves along specific crystallographic planes (slip planes). All atoms in slip deformation displace the same amount of distance, and the orientation of the crystals maintains equal.

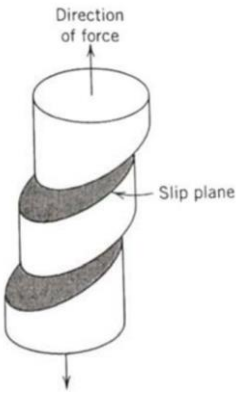

Figure 15: Slip system on a crystal (Tamimi, 2013).

Within polycrystalline materials, a crystal (grain) is not able to deform plastically alone, remaining in contact and accommodate the shape change of its neighbours. Consequently, during plastic deformation, the grains take preferential orientation which is defined as the texture of the material. Macroscopically, the texture and microstructure evolution during plastic deformation is observed by the variation of the mechanical properties for different directions. The phenomenon is called anisotropy. For sheet metals, it is usual do characterize the anisotropy based on the mechanical behaviour exhibited at three orientation regarding the rolling direction, namely, 0º, 45º and 90º as represented in figure 16.

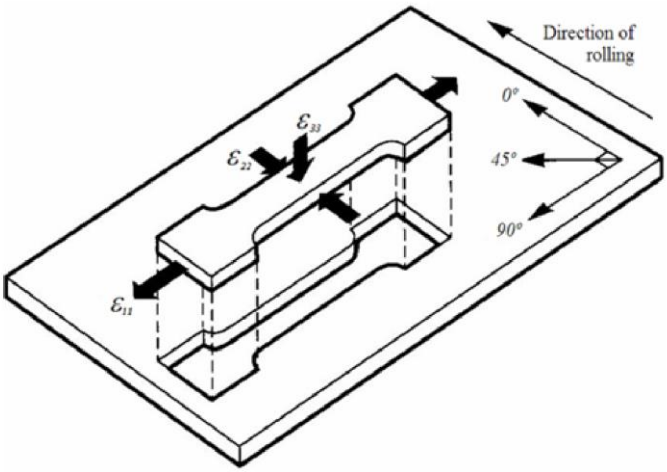

Figure 16: Deformations of a samples in three different angles with the rolling direction.

During plastic deformation, the materials register strain hardening which is the ability of a material to strengthen itself when employed strain into it.
While deforming some aluminium alloys, below its recrystallization temperature, dislocations movements are added to crystalline structure of the material. The increase of the number of dislocations is directly connected with the strength of the material. When deforming strain hardenable alloys, a lot of dislocations are created, leading to interference regarding opposing movements, and consequently making the material stronger.

Metal forming processes have been used through times in metalworking. These processes are characterized by applying load to the metal, changing its shape. These processes do not involve removing material as machining. There are many types of metal forming processes, like rolling, extrusion, forging, indenting and others which exert tensile / compressive / shear stress into the metal. The mentioned processes intend to alter the shape of the metal and modify their crystalline structure.

2.4.1. Rolling

There is a huge number of rolling processes. It can vary from the most common, flat rolling, to more complex processes like roll forming, bending, ring rolling and others. Flat rolling (named rolling from now on) is the elected way to apply plastic deformation to the aluminium samples. Even so, there are 2 types of flat rolling, cold and hot rolling.

As the name indicates, these two types of rolling differ in the temperature in which they are processed. Cold rolling is when the rolling process is done at a lower temperature than the RT (recrystallization temperature) of the material. Hot rolling, on the contrary, rolls the metal sheet above its RT. Cold rolling, however, induces plastic deformation on a material changing its properties on the spot, unlike hot rolling in which the recrystallization is occurring during the process and only after the process it starts to stabilize and to configure its structural identity.
There are different needs in the metal specifications, thus, when manufactured, these two processes might be used to secure their fulfilment.
The concept behind sheet rolling is simple (figure 17). A sheet of metal goes through a gap between the rolls on the rolling mill altering its form and reducing its thickness.

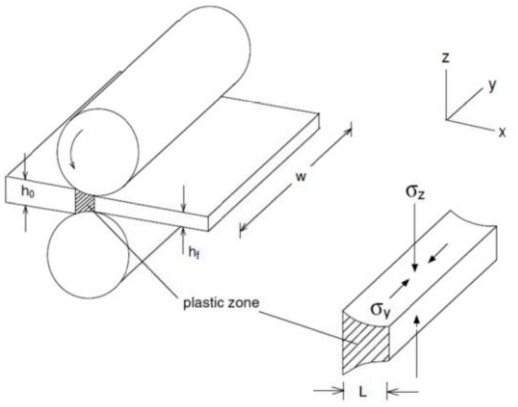

Figure 17: Rolling process and deformation induced to the sheet metal (Tamimi, 2013).

Despite being a simple process, there are a lot of technical details that, when adjusted, produce different effects on the sheet metal. The main components of a rolling mill are its rolls. The characterization of these rolls defines what happens to the metal in contact with them. Milling rolls can vary in size and velocity which provoke distinct plastic deformations. Also, the distance of the gap between the rolls and the thickness of the material constitute another key factor when analysing the deformation of the metal. Other aspects like the friction between the metal and the rolls may constitute an effect on the material since phenomena like slipping or gripping may affect the quality of the process.
During rolling, the sheet metal decreases its thickness as it passes through the rolls. This thickness reduction follows an increase in the velocity of the sheet metal. The deformation through the width of the metal sheet is ignored, the length and thickness of the metal are the indicators of the strain induced. The configuration between rolls origins two types of rolling processes: conventional (or symmetric) and asymmetric.
Conventional rolling (figure 18) happens when the two rolls are equal, that is, both have the same diameter and velocity. This one is the standard process of rolling and it induces plane strain deformation in the samples.

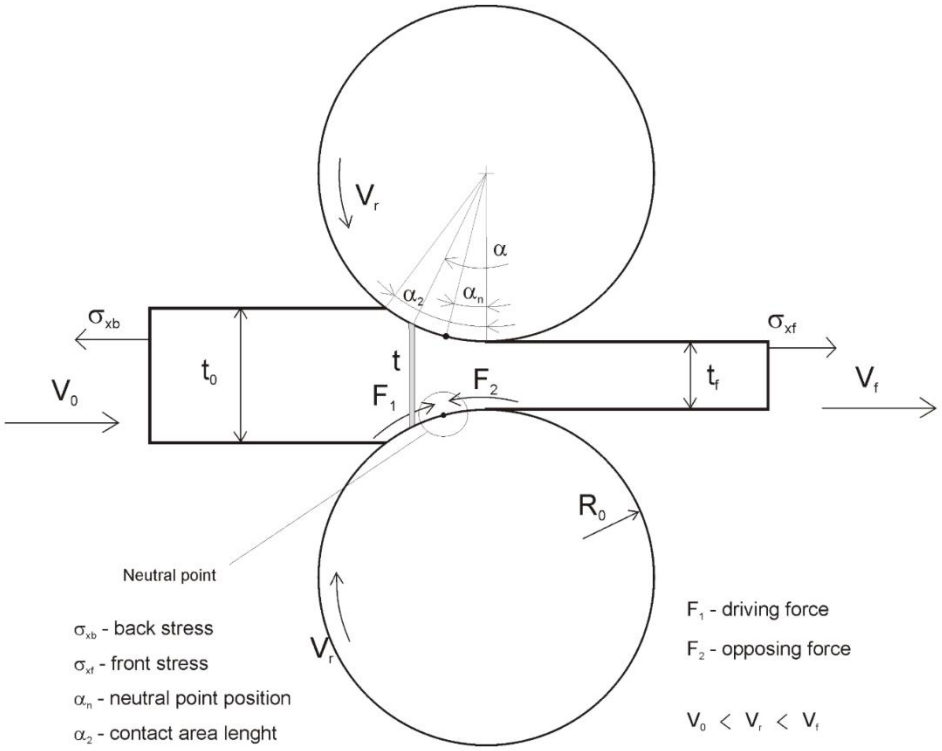

Figure 18: Conventional rolling parameters (Avitzur, 1983).

Unlike CR (conventional rolling), ASR (asymmetrical rolling), (figure 19) does not have the same specifications on both rolls. A change in their diameter and / or velocity drives the metal through the gap between them in a slightly uneven way. Originated from this process is the induction of an additional shear strain into the metal.

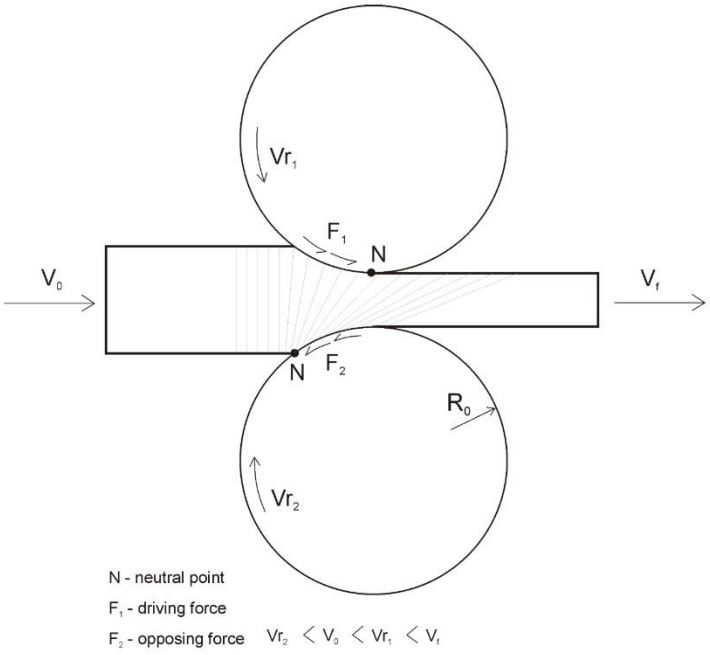

Figure 19: Asymmetrical rolling (Simões, 2008).

When the rolls parameters differ from each other, the neutral points (points where the circumferential velocity of the rolls is equal to the velocity of the sheet movement) become asymmetric resulting in the asymmetrical displacement of the material, creating a shear strain through the sheet thickness. Any difference in velocity or size of the rolls is enough to cause a difference in the rolling symmetry.
Currently, asymmetrical rolling is being investigated as an alternative to conventional rolling. A search for materials with improved mechanical properties is the central point for developments in this field (Mirzakhani & Mansourinejad, 2011; Zhou et al., 2018).

2.5. Heat Treatment

As mentioned earlier, some aluminium alloys are heat treatable. In this kind of alloy, it is possible to control the formation of precipitates. There are a variety of heat treatment methods that cause different changes to the structure and mechanical properties of most metals.

The worked aluminium (AA6061) falls in this category.

2.5.1. Annealing

Annealing is a type of heat treatment commonly applied after cold working to increase the ductility and formability of the material. The process consists in exposing the metal to high temperature, keeping it at that temperature for an extended amount of time, and then slowly cooling it at room temperature.
When cold worked, metals develop residuals stresses that affect its formability. The annealing process is frequently used to complement the development of certain alloys. It is done at relatively low temperatures in order not to affect the improvements of cold working.
Recrystallization is a phenomenon that happens when a heat treatment is applied. New grains that compose its microstructure are created, in formerly cold-worked materials, disassociated with strain.

2.5.2. Solution Heat Treatment

Solution heat treatment is a heat treatment in which the material is heated at high temperatures corresponded to a solubilisation range for a period and quenched, cooling it rapidly. In this process all solutes are dissolved, forming a single-phase solid solution. Normally this process precedes a precipitation heat treating.

2.5.3. Aging

The age hardening (also called precipitation hardening) of aluminium opened a path for endless possibilities by altering the microstructure of the metal. Rapidly, different combinations of temperatures and times of exposure started to be tested by the scientific community, therefore, the era of aluminium came to the spotlight (Aruga et al., 2015; Bahrami et al., 2012; Berneder et al., 2017; Polat et al., 2015; S. Zhang et al., 2019).

Aluminium alloys are composed by different elements, atoms of these elements, alongside with the aluminium atoms, form the crystalline structure of the metal which strengthens it due to the difference in size between them, positioning and density.

When submitted to distinct temperatures the atoms re-arranged themselves through the based metal, and, when quenched rapidly, stay trapped in those locations.

After a while, the atoms adhere one to another forming a diverse crystal structure. This is called 2nd phase, or precipitate. This offers a more cohesive resistance to deformation, making the material more resistant.

The process of natural age hardening occurs at room temperature. It was discovered by accident when Alfred Wilm, frustrated by not being able to alter aluminium by quenching, like steel, left the aluminium samples previously quenched at room temperature resting until the next day. When Alfred checked the properties of the samples in the next day, he was shocked with the results. The strength of the samples increased overnight.

There is a limit to how much precipitates can be formed at room temperature. It created a precedent that would be one of the main boosters for the aluminium economy, though.

Artificial aging does not occur at room temperature. To form precipitates, some alloys need to be subjected to certain temperatures during periods of time.

Alloys behave differently to the two variables, temperature and time. Generally, an artificial aged alloy increases its strength through time until it reaches a maximum value. After that, the strength starts decreasing. In order to improve the properties of a metal, it is essential to determine that balance between the variables. Different temperatures (Bahrami et al., 2012; Polat et al., 2015) cause altered behaviours in the properties of the material (figure 20).

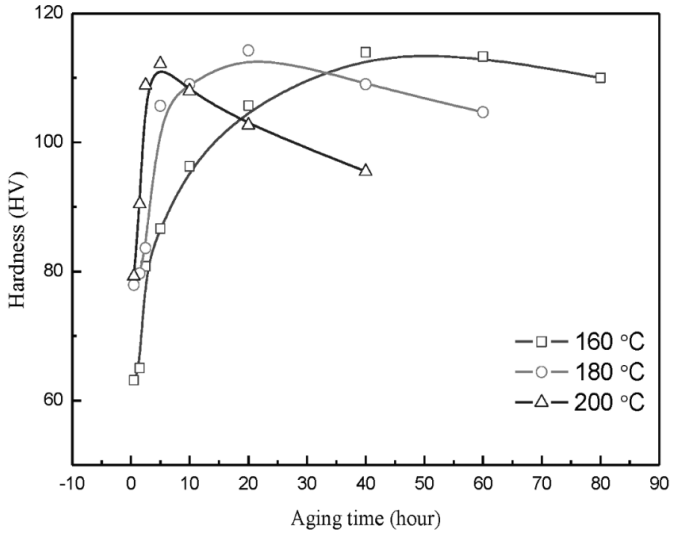

Figure 20: Influence of aging temperature and time in mechanical properties of AA6061 alloy (Polat et al., 2015).

3. Experimental Procedure

This chapter shows in detail the experimental procedure, from the as-received material assessments to the last tests conducted on the processed aluminium alloy.
Tensile and hardness tests are conducted to evaluate the mechanical properties of the aluminium samples. These tests are essential to extract the stress-strain behaviour of the material and the values of hardness, respectively.
The trials of material enhancement were done using heat treatments and rolling, requiring specific furnaces and machinery.

3.1. Data gathering methods

3.1.1. Mechanical properties characterization

Tensile tests are one of the most complete method of characterization of the material's mechanical properties. Throughout this work, due to some technical problems, two group of equipment were used in the present work as described below:

1) Standard uniaxial tensile tests were conducted with a SHIMADZU Autograph Machine (maximum capacity 100 kN, figure 21). The test speed was adjusted in order to produce a strain rate equal to 10^{-3}/s. In order to determine the strain, a digital image correlation (DIC - a metrology system manufactured by GOM (see figure 22) was employed to measure the displacement field. The ARAMIS-5M software was used to post-processing the strains from optical images.

Figure 21: SHIMADZU Autograph Machine.

Figure 22: ARAMIS adjustable model by GOM.

The cameras and lightning above allow a good capture of the samples' images subjected to traction by the tensile test machine. The 3D measurement was made by using two cameras that captured one image per second during the test. For the correct reading of the images (figure 23), the cameras had to be calibrated and the samples painted as described in the technical documentation.

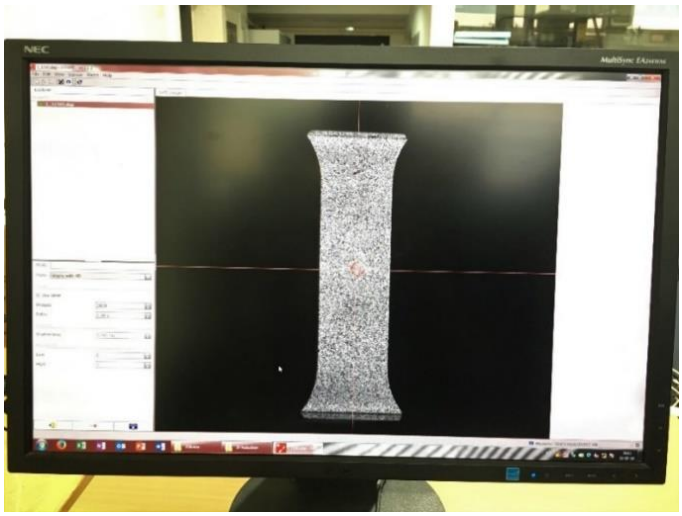

Figure 23: ARAMIS software for image reading/processing.

2) For the second part of the work, uniaxial monotonic tests were performed in tension at room temperature using a Shimadzu Autograph Machine with maximum load capacity of 50kN. In this case, the equipment was coupled with a video extensometer Messphysik ME 46 to measure the strain (figure 24).

Figure 24: Shimadzu Autograph Machine (maximum load capacity of 50kN) and Video Extensometer Messphysik ME 46.

3.1.2. Sample preparation and sizes

As mentioned, the samples had to be prepared to allow correct readings from ARAMIS. At first, a white coat of paint was applied to the samples; afterwards, black paint was sprayed into it (figure 25), making it a grayscale image that the software traces, calculating the strain created during tensile testing.

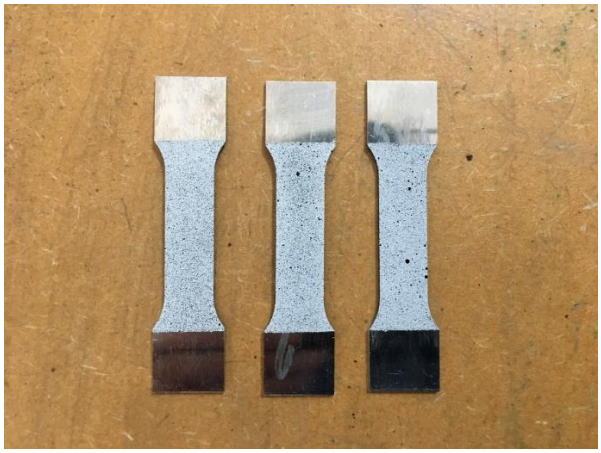

Figure 25: Prepared samples for tensile tests.

The samples were machined in a CNC machine by a technician of the department. The parameters of the samples were chosen (according to the ASTM E8 standards) (figure 26).

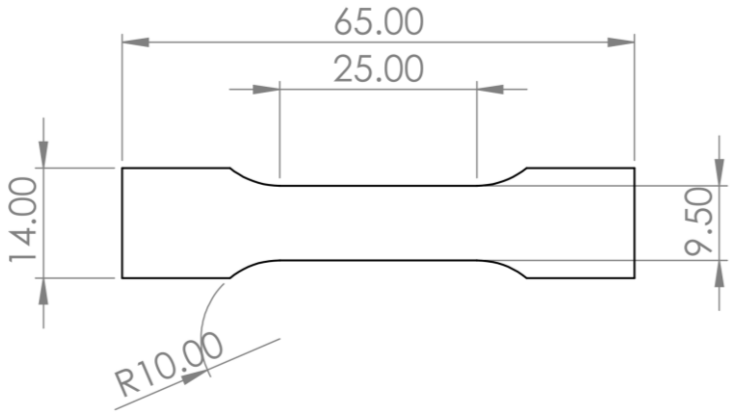

Figure 26: Dimension of the tensile test samples.

3.1.3. Hardness tests

Hardness tests were a key process to evaluate and compare the mechanical properties of the different samples of aluminium. It proved to be an effective alternative to the time-consuming tensile tests, for intermediary operations.

The hardness test used in this work is Vickers (HV) and was applied to several steps of this investigation.
The equipment used to measure the Micro Vickers hardness is the Shimadzu HMV-2000 (figure 27).

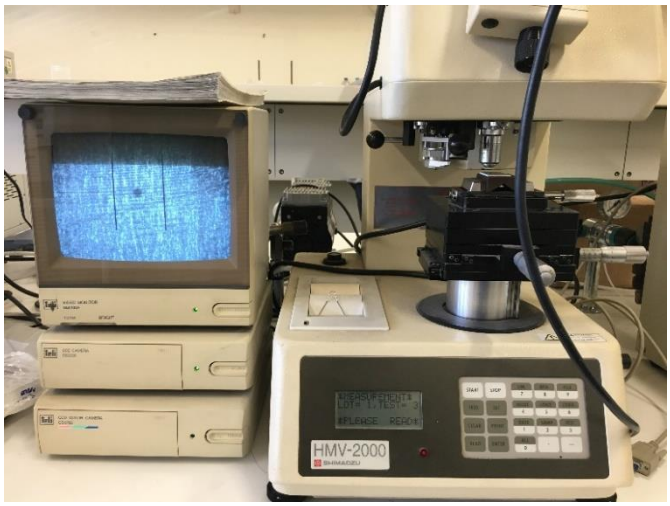

Figure 27: Shimadzu HMV-2000.

An indentation with a load of 100 gf during a period of 15 times was used (figure 28).

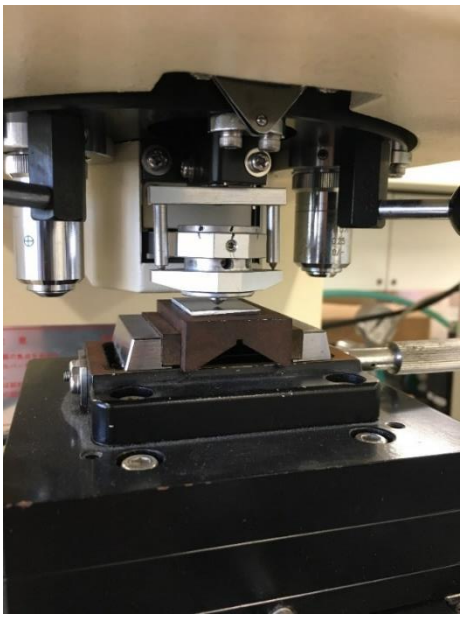

Figure 28: Close-up of the sample indentation.

As referred in the literature review, a diamond shaped indentation is printed in the sample. The dimensions of the mark are processed by software exporting the correspondent Vickers Hardness (figure 29).

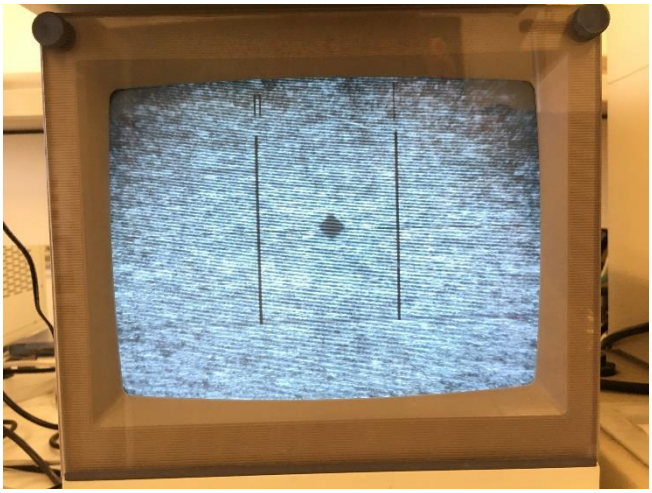

Figure 29: Observed diamond-shape indentation.

3.1.4. EBSD Analysis

The EBSD analysis is a technique essential to investigate the evolution of the aluminium alloy texture through different processes.
The crystallographic orientation (texture) was measured in the as received material and after rolling using a HR-FE SEM Hitachi SU70 equipment operating at 25 kV and equipped with a Quantax Cryst Align EBSD system from Bruker (figure 30).

Figure 30: HR-FE SEM Hitachi SU70

3.2. Material processing

The main processes used in this work to enhance the alloy are Heat Treatments and Strain Hardening. However, other support processes are necessary to complete the study as grinding and polishing.

3.2.1. Grinding and Polishing

Even though grinding and polishing are not a core processes, meaning that, it doesn't, directly, change material properties, it is important to support the others.
In order to obtain the best quality of the indentation, the samples must be well-polished, in a way that the contact surface has a mirrored surface. That way, the shape of the indentation will be easier to spot, allowing better readings.
The rolling process also requires polished sample. The idea is to polish the side faces of the aluminium samples before rolling, so that, regarding Asymmetric Rolling, the shear strain induced can be measured.
Several grinding foils with different grit (800, 1200, 2000, 4000) were used in Struers RotoPol-21 equipment allowing the intended final mirrored finishing (figure 31).

Figure 31: Unpolished sample (left) vs polished sample (right).

3.2.2. Rolling

Rolling is one of the two main processes responsible for changing/enhancing the aluminium properties, alongside heat treatments.
In this dissertation, Symmetrical Rolling and Asymmetrical Rolling (ASR) are explored. From this point on, symmetrical rolling is be labelled as Conventional Rolling (CR). Regarding Asymmetric rolling, there are two combinations of roll's velocity ratio that are compared, namely 15/11 RPMs and 15/5 RPMs. The diameters of the rolls are identical.
Other parameters such as the rolling routes, either continuous or reverse, are also accounted for in the rolling process. These routes are detailed in the following chapter.
The rolling mill used to roll the samples is the one belonging to the materials lab at DEM-UA (figure 32).

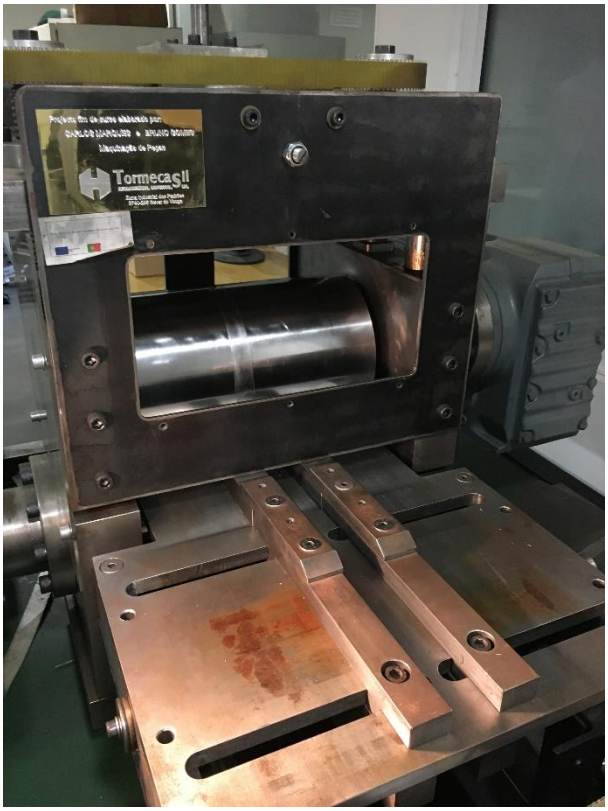

Figure 32: Asymmetric rolling mill used in the present work.

3.2.3. Heat treatments

Heat treatments were conducted with two objectives: i) before rolling to do solubilisation of the precipitates; ii) after rolling to do annealing.
The solubilization heat treatment start at room temperature, increasing steadily until reaching the solubilisation temperature followed by a period of waiting until the precipitates are dissolved. In the annealing heat treatment, the samples are introduced into the furnace at the desired temperature and the heating stage is skipped
These heat treatments were conducted in home-made furnaces of the Mechanical Engineering Department.

3.3. As received material assessment AA6061-T6

Initial tests were conducted to determine the properties of the studied aluminium in the as received state, namely AA6061-T6. Hardness and uniaxial tensile tests were made from a sheet metal with thickness of 2.10 mm.
Stress-strain curves, Vickers Hardness, anisotropy and texture details are the outputs from the tests mentioned above. The mechanical composition of the alloy was given by the supplier (table 4).

Table 4: Chemical composition of the as received material (except aluminium).

Chemical Composition (%)									
Si	Fe	Cu	Mn	Mg	Ni	Cr	Zn	Ti	Others
0.59	0.48	0.25	0.11	0.94	0.00	0.23	0.11	0.10	0.15

3.3.1. Hardness

First measurements of the AA6061-T6 were made, starting with Vickers Hardness.
To validate the measured hardness values, the degree of surface polishing was tested. Three samples with different surface finishes were considered: not polished, superficial polished and deep polished. Deep polished is the reduction of the sample thickness by half, and the superficial polishing is in the middle of the two extremes (table 5).

Table 5: Values of Hardness for different polished finishes.

	Hardness (HV)		
	Superficial Polished	Deep Polished	Not Polished
	110	85.5	96.6
	110	113	103
	105	111	94.4
	103	106	97
	105	105	96
Mean	106.6	104.1	97.4

Five trials were carried out for each tested sample. It is shown that the degree of polishing does not interfere with the properties of the aluminum. However, polishing is essential to obtain reliable readings. The more the surface is finely polished, the more the indentation is visible, and the more accurate the measurements of its shape are (figure 33).

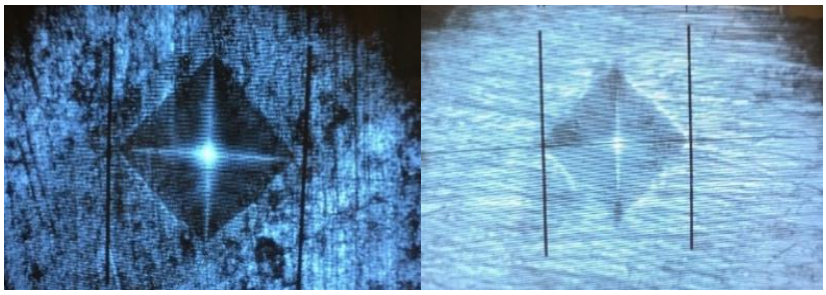

Figure 33: Microscopic images of Vickers diamond indentation.

3.3.2. Characterization of AA6061-T6

Defining the mechanical properties of the AA6061-T6 is a crucial step for the rest of the investigation. The first set of tensile tests characterize the complete mechanical behavior of the worked alloy. To this end, three groups of samples were prepared regarding to the rolling direction (RD), namely the sample were cut at 0º, 45º and 90º from RD. The stress-strain curves of each group are presented in figures 34, 35, 36.

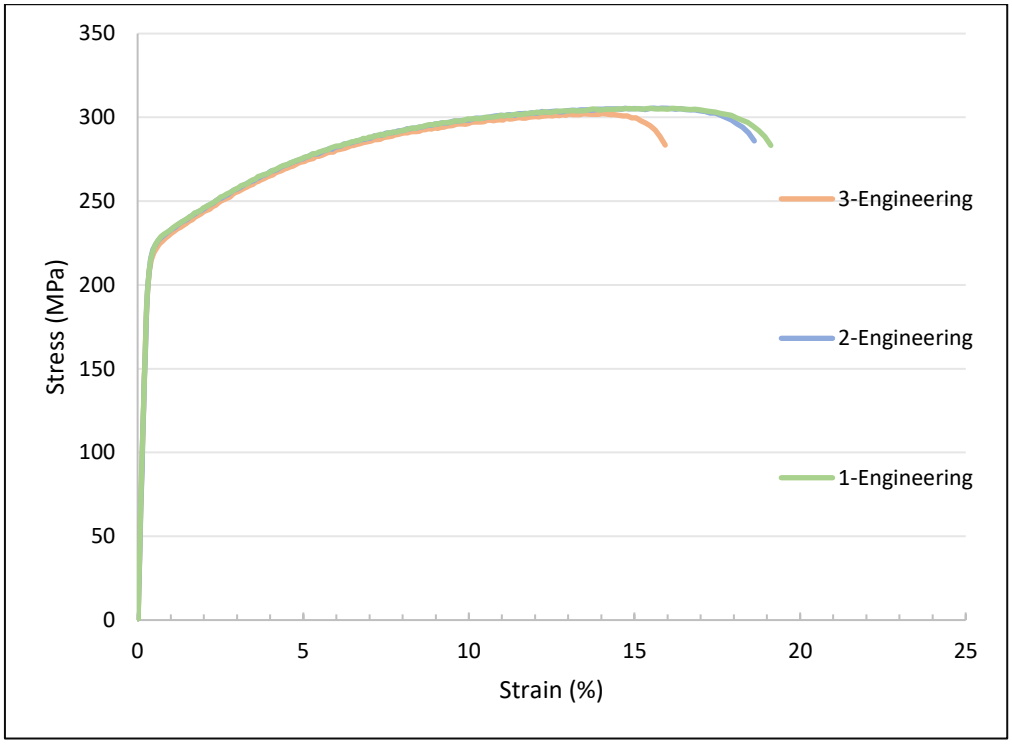

Figure 34: Stress-strain curves of 0˚ rolling direction.

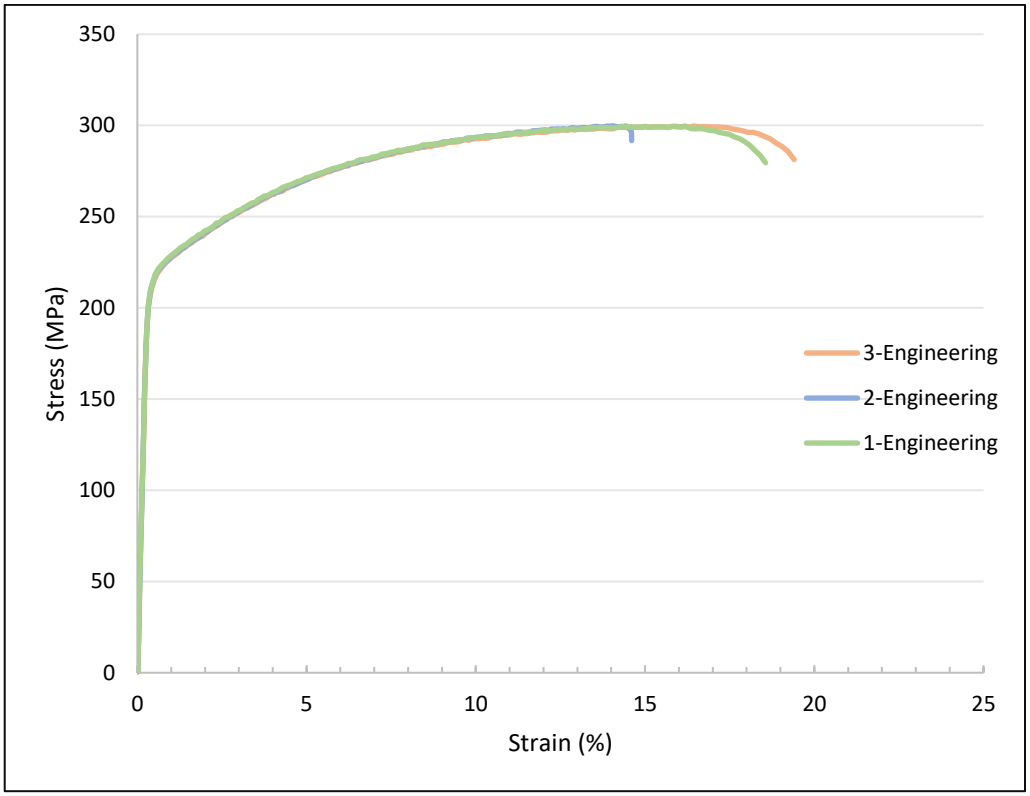

Figure 35: Stress-strain curves of 45˚ rolling direction.

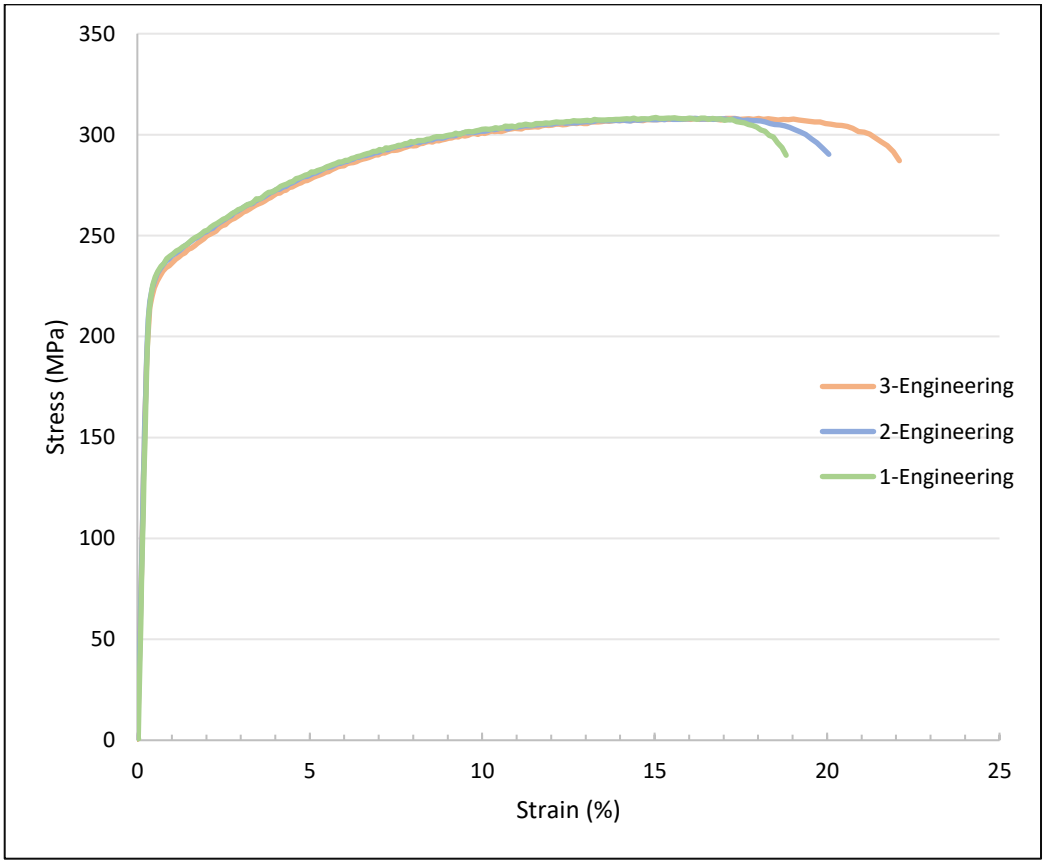

Figure 36: Stress-strain curves of 90˚ rolling direction.

Three samples of each rolling direction were tested. All the results obtained were summarized in the following tables (tables 6 and 7).

Table 6: Mechanical Properties of AA6061-T6.

Rolling Direction	Trials	Elasticity Modulus		Yield Strength		Tensile Strength	
		(GPa)	Mean	(MPa)	Mean	(MPa)	Mean
0°	1	73.07	74	222.65	223	305.39	304
	2	72.63		226.24		305.51	
	3	74.96		219.88		302.29	
45°	1	74.49	74	215.98	217	299.59	300
	2	74.48		217.75		299.82	
	3	73.70		216.98		299.71	
90°	1	75.59	75	231.49	229	308.50	308
	2	73.63		229.85		308.03	
	3	75.20		224.57		308.03	

Table 7: Mechanical Properties of AA6061-T6 (continued).

Rolling Direction	Uniform Elongation		Elongation at Break		Anisotropy			
	(%)	Mean	(%)	Mean	r-values	Mean	n-values	Mean
0°	15.49	15.03	19.12	17.89	0.59	0.59	0.18	0.18
	15.57		18.62		0.59		0.18	
	14.04		15.93		0.59		0.18	
45°	15.82	15.43	18.56	17.53	0.56	0.56	0.18	0.18
	14.04		14.61		0.56		0.18	
	16.44		19.41		0.56		0.18	
90°	15.03	15.77	18.81	20.32	0.75	0.75	0.17	0.17
	16.10		19.88		0.74		0.17	
	16.17		21.92		0.76		0.18	

The results for the preliminary material characterization concluded that the Modulus of Elasticity is practically the same (the larger gap is circa 1.3 GPa) in any direction of the material. Furthermore, the Yield Strength differs slightly (circa 12 MPa in magnitude) when different orientations are considering. The 90º orientation proves to have the highest yield stress and the lowest yield stress is the recorded for 45º orientation. The anisotropy coefficient is shown in figure 37.

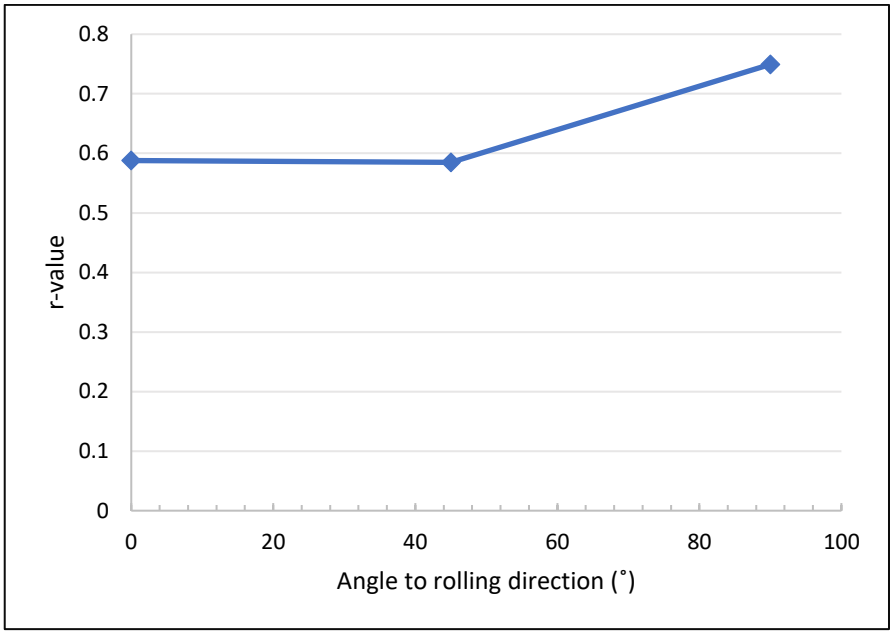

Figure 37: Anisotropy curve of the as received material.

Although the initial material was characterized for the three rolling directions, only 0° direction is considered for the tensile tests after rolling operations. Such fact is due to the constraints of the rolling mill. In the current state, the rolling mill does not support large sizes of the specimens that are necessary in order to cut samples at 45° and 90° from the rolling directions.
EBSD analysis of the samples was made to confer the texture of the initial material.
The key provided shows the orientation of the grains (figure 38). This key is the same for every EBSD picture included in this document.

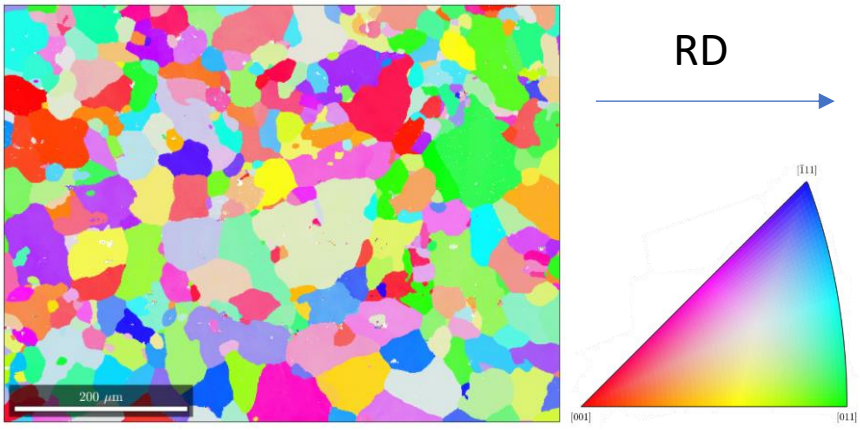

Figure 38: AA6061-T6 texture and respective key.

The average grain size is around 50 µm.
In order to investigate the preferred orientation of the grains, the pole figure corresponded to {111} and the 3 sections of ODFs corresponded to φ_2 0º, 45º and 65º were used (figure 39).

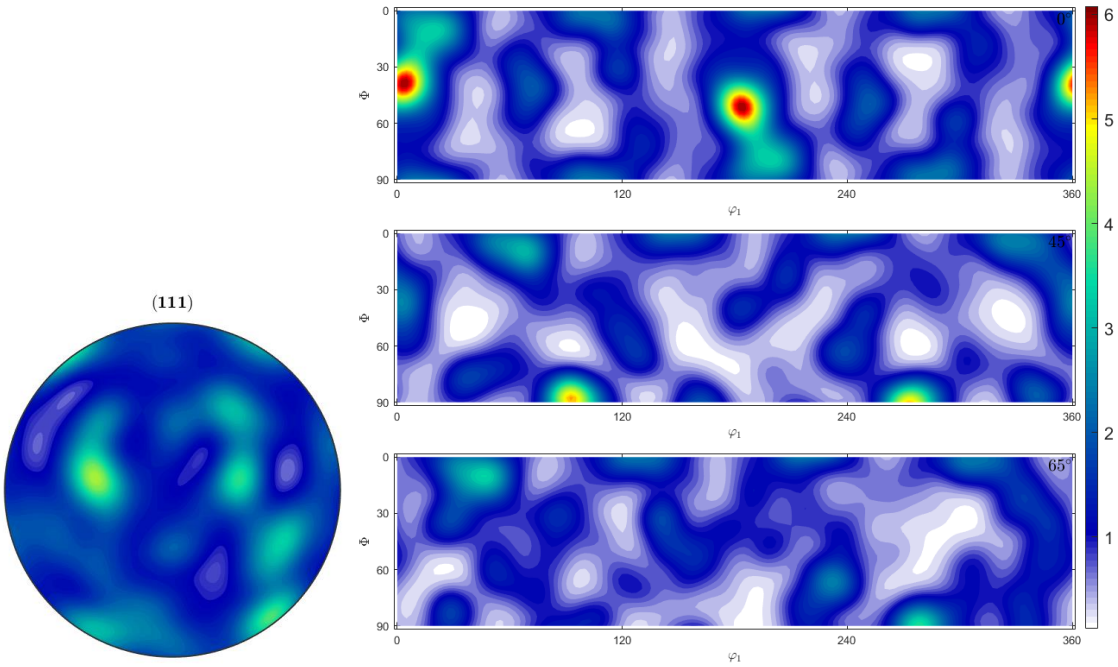

Figure 39: PFs and ODF's of AA6061-T6, as received.

The most predominant texture component in the observed samples is the Goss {011} <001>. Cube {001} <100> is another recrystallization type texture component found in the ODFs. The used keys were the ones presented in figures 13 and 14.

No evident deformation texture component is shown, therefore, the results from the microscopy are in accordance with the T6 temper applied to the AA6061 aluminium.

3.4. Heat treatment before rolling

As the aluminium used until this point is already thermally tempered, it is undertaken a heat treatment to revert the AA6061 its original properties. Only from that point on, it makes sense to apply changes to the material in order to improve it.
The combinations of temperature and time were defined according to previous work of (Schmid et al., 2019; Xu et al., 2019; X. Zhang et al., 2020).

A representation of the effects of Solution Heat Treatments is referenced by Zhenhai Xu et al (figure 40).

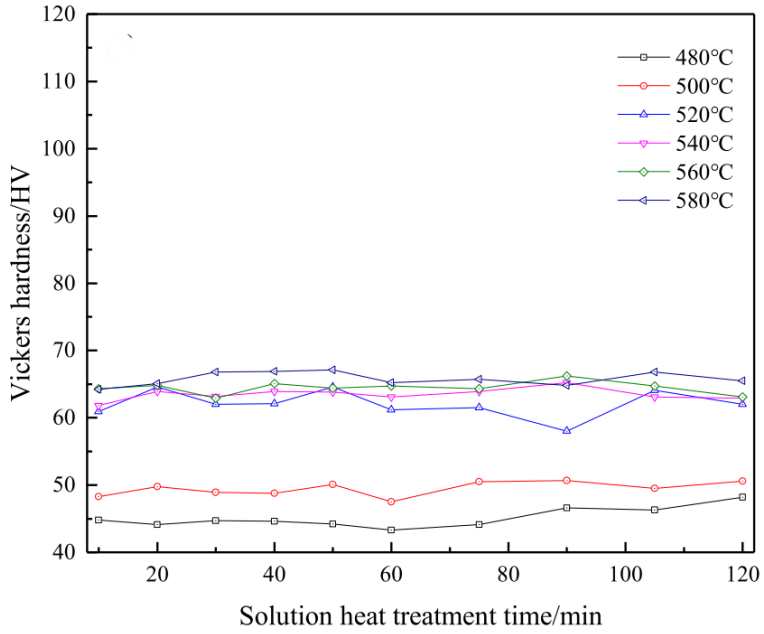

Figure 40: Effects of solution heat treatment in AA6061 hardness (Xu et al., 2019).

Two solution heat treatments were carried on, denominated as SHT1 (Solution Heat Treatment 1) and SHT2 (Solution Heat Treatment 2), corresponded to 550ºC/30min and 530ºC/2h, respectively. Schematic diagram is shown in figure 41.

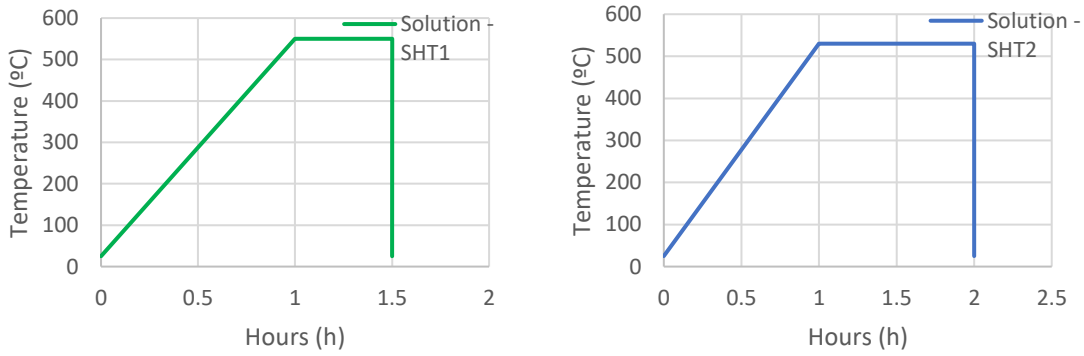

Figure 41: Plot of SHT1 and SHT2.

The diagrams show an increase from 25ºC till the desired temperature during an interval of 1 hour, approximately. This section of the heat treatment represents the time the furnace needs to reach the pic temperature.

3.4.1. Effects of natural aging after the solubilisation heat treatments

Due to the phenomenon of natural age hardening, properties vary from the moment they are quenched until they stabilize. To track down this window of time, hardness tests were conducted to the SHT2 combination.
The samples were observed during an interval of 71 hours after quenching (figure 42).

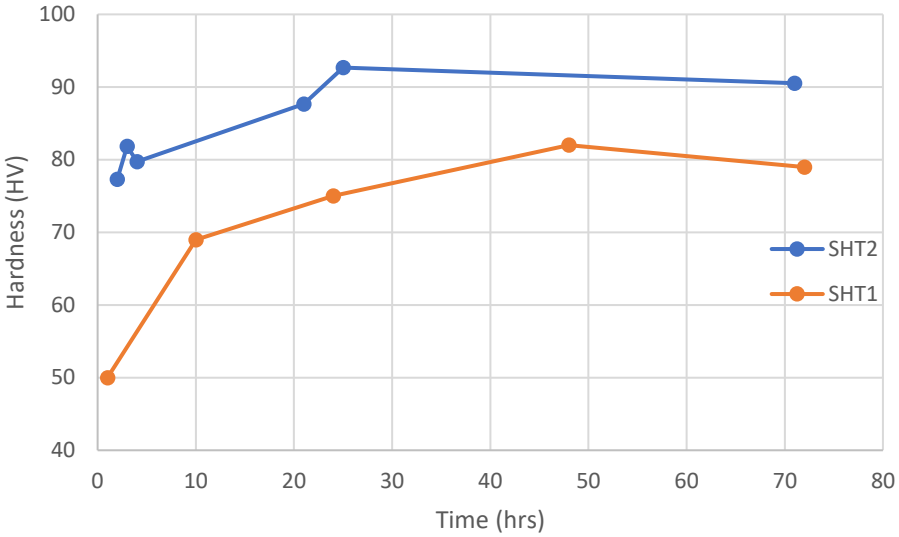

Figure 42: Effects of age hardening after SHT1 and SHT2 in the material's hardness.

As it is visible in the presented curve, the hardness values become more stable around the 2 days mark because of natural age hardening. Due to that fact, it was established a waiting time of 3 days before the cold working of the samples.

3.4.2. Testing solution heat treatments

The same process of rolling will be used for the two sets of solubilized samples (SHT1 and SHT2). Different rolling methods will be covered in an ensuing chapter; therefore, the data acquiring will be presented as one in the same chapter, highlighting the main variances between the two.

3.5. Rolling

Testing the effects of different rolling setups is the main differentiator regarding properties enhancing. As mentioned in the previous chapter, rolling configurations will be tested for both (SHT1 and SHT2) pre-rolling heat treatments combinations.

3.5.1. Route processing

There are 2 types of rolling that will be tested, conventional symmetric and asymmetrical. Reduction per pass, velocity of the rolls and rolling direction are the variables studied to check whether it is or not possible to enhance the mechanical properties of a recrystallized AA6061.

The conventional rolling will be performed with a 15 RPMs velocity for both rolls. It is in the asymmetrical rolling that new routes are taken. Two velocity combinations are tested, namely: i) one under 15 RPMs and 5 RPMs for the upper and lower rolls respectively; ii) the other range of velocities are 15 RPMs and 11 RPMs.

The routing of the asymmetrical rolling samples, whether continuous or reversed, constitute another variable to the process (figure 43).

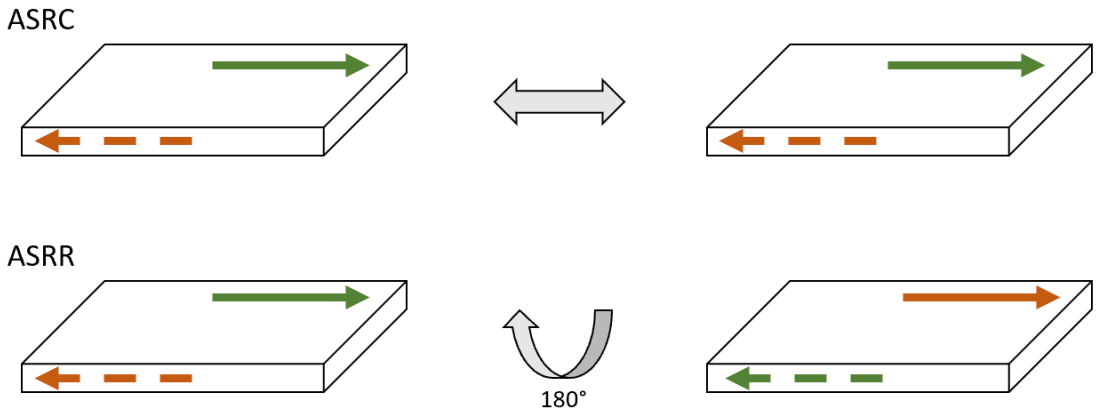

Figure 43: Route of asymmetric rolled samples, ASRC and ASRR.

4. Results and Discussion

This chapter presents the results obtained in the experimental procedure, as well as a discussion of those results and relevant features.
Several tests were made during the investigation period. The continuous evaluation of the results led to a set of decisions that converged into final conclusions.
Important factors regarding the performance of the material and respective equipment is presented here.

4.1. Step 1 – Solubilization heat treatments and rolls velocities.

The purpose of the first step was to evaluate the SHT and the factors employed to create the asymmetry of the rolling process. The working diagram is summarized in figure 44. Since these are initial tests, one of the main objectives was to validate the measurements and avoid any future problems. The used reduction per pass was 20%.

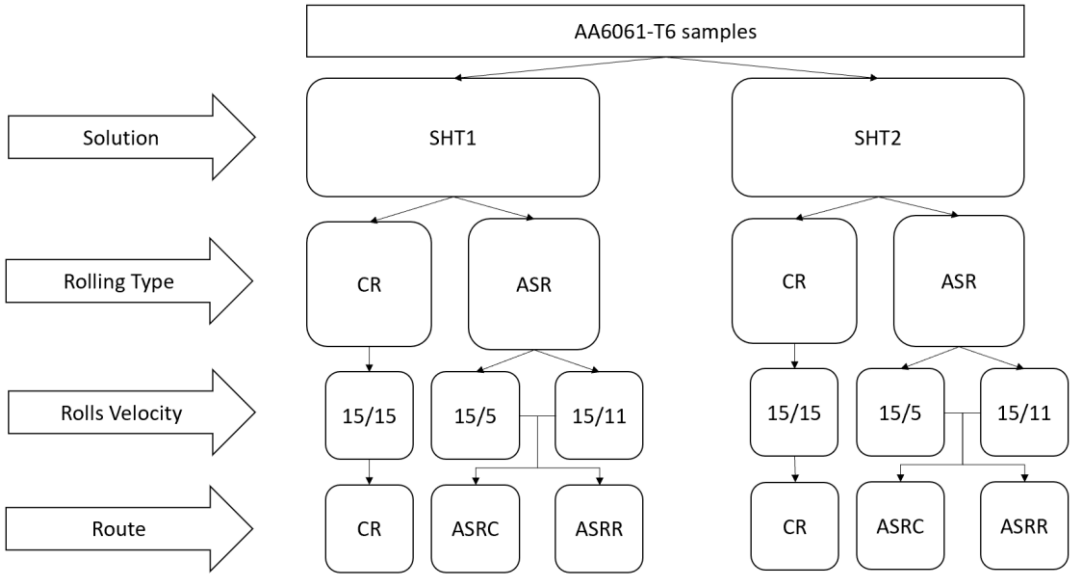

Figure 44: Schematic of carried out processes (step 1).

Three samples for each test were prepared to ensure the quality of the data. As a result, about twenty samples were baked at the same time for each solubilisation process.
After quenching, the samples were stored for, at least, three days before rolling. As concluded in chapter 3.4.1., this interval of time helps the material to stabilize. This action was taken to minimize the variance of the aluminium properties in the rather large amount of upcoming hardness and tensile tests. The hardness tests values are subjected to validation by comparing them to the data acquired from uniaxial tensile tests. Hardness tests for each SHT were done registering the following values (table 8 and 9).

Table 8: Vickers hardness for rolled samples after SHT1.

SHT1			
Velocity (RPM's)	Route	Hardness (HV)	Trial
15/15	CR	106.4	1
		116.6	2
		122.2	3
15/5	ASRC	105.6	1
		99.88	2
		102.1	3
	ASRR	120.4	1
		126	2
		110.6	3
15/11	ASRC	102.5	1
		105.6	2
		123.4	3
	ASRR	-	1
		121.4	2
		122	3

Table 9: Vickers hardness for rolled samples after SHT2.

SHT2			
Velocity RPM's	Route	Hardness (HV)	Trial
15/15	CR	134.2	1
		132.8	2
		138.2	3
15/5	ASRC	128.8	1
		136.2	2
		134.6	3
	ASRR	106.4	1
		121.8	2
		135.2	3
15/11	ASRC	137	1
		138.2	2
		141.2	3
	ASRR	139.2	1
		137	2
		138.4	3

The Vickers Hardness values in the table 7 are a result of a mean of 5 measures for each trial.
The magnitude of the values ranges from 100 to 125 HV.
The Vickers Hardness for AA6061-T6 is around 107HV (according to "ASM Material Data Sheet", 2019). Therefore, the samples did not register a significant growth in strength compared to the previous alloy.

There are a lot of variance amongst the values of hardness even for the same sequence. CR samples differ in about 16 HV. One of the ASRR1 sample was damaged during the rolling process, which explains the absence of a value in table 7.

The SHT2 after rolling produced higher values of hardness than the ones observed in AA6061-T6 samples (table 8). The magnitude of the values is in a range of 130 to 140 HV. In this set of results, the ASR is best fit regarding hardness enhancing. Considering only ASR (15/11), the continuous and reverse configurations show similar values, around 138-139 HV. These values represent an improvement over 30HV from the as received material.
The results from the hardness test were not conclusive. The inconsistency of the results can be attributed to different factors, such as:

i) the conditions of the furnace in which the heating process was done, and the damage sustained by the samples when rolling;
ii) ii) the excessive number of samples baked at the same time affect the heat distribution within the furnace, causing the heated samples to suffer SHT in diverse conditions.

For 15/5 RPMs, a large amount of plastic work was released during the process, leading to the heating of the sheet, and consequently, damaged the surface of the sample. In figure 45 is presented the upper roll of the mill where a thin layer of aluminium pertaining to the sample can be observed.

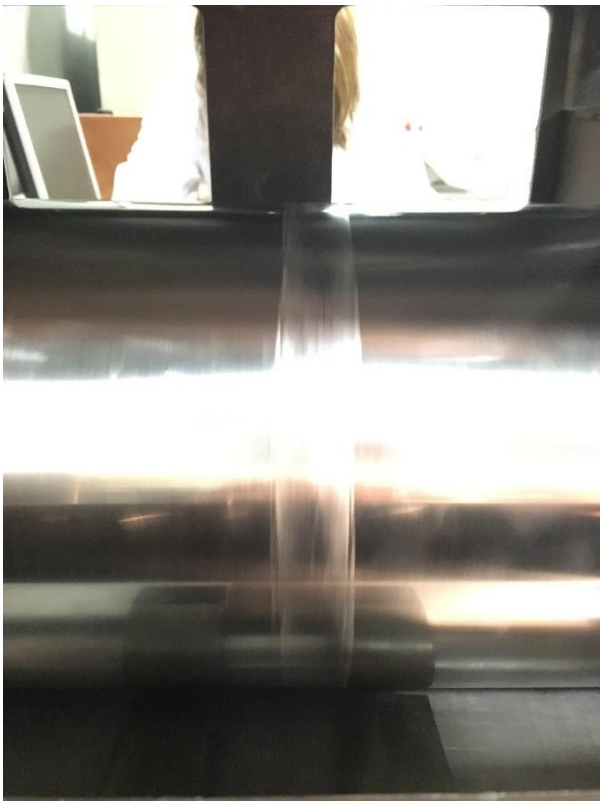

Figure 45: Effects of ASR (15/5) on the roll surface of the mill.

To validate the hardness tests and to obtain detailed information about the samples' strength, uniaxial tensile tests were done.
The mechanical properties obtained from the stress-strain curves' analysis are presented below (tables 10 and 11).

Table 10: Mechanical characterization of the rolling sequences after SHT1.

SHT1				Yield Stress (MPa)	Maximum Stress (MPa)	Elongation at Break (%)
CR	15-15	CR	1	289.35	298.00	4.38
			2	340.42	350.45	4.98
			3	338.69	350.80	4.95
ASR	15-5	C	1	259.71	282.18	2.42
			2	290.59	297.75	3.10
			3	286.13	294.06	2.15
		R	1	324.81	342.09	2.22
			2	298.59	313.39	3.02
			3	-	296.48	2.98
	15-11	C	1	283.87	293.62	3.99
			2	304.40	311.74	4.04
			3	343.79	355.70	4.58
		R	1	-	-	-
			2	328.15	339.86	4.78
			3	340.47	352.41	4.81

Table 11: Mechanical characterization of the rolling sequences after SHT2.

SHT2				Yield Stress (MPa)	Maximum Stress (MPa)	Elongation at Break (%)
CR	15-15	CR	1	372.49	385.46	6.31
			2	369.18	383.91	5.35
			3	371.41	388.94	5.03
ASR	15-5	ASRC	1	298.30	305.06	3.58
			2	367.37	384.48	5.20
			3	349.37	365.82	5.28
		ASRR	1	366.29	384.25	6.43
			2	344.38	359.73	5.74
			3	366.99	382.36	6.06
	15-11	ASRC	1	378.10	395.19	5.13
			2	384.14	398.70	5.63
			3	360.15	373.58	3.86
		ASRR	1	383.22	398.21	5.58
			2	382.11	397.18	5.25
			3	387.17	400.60	6.07

Mechanical properties were obtained through the data analysis of the ARAMIS and Shimadzu inputs. The values presented in the tables were extracted from the stress-strain curves of the material (figure 46).

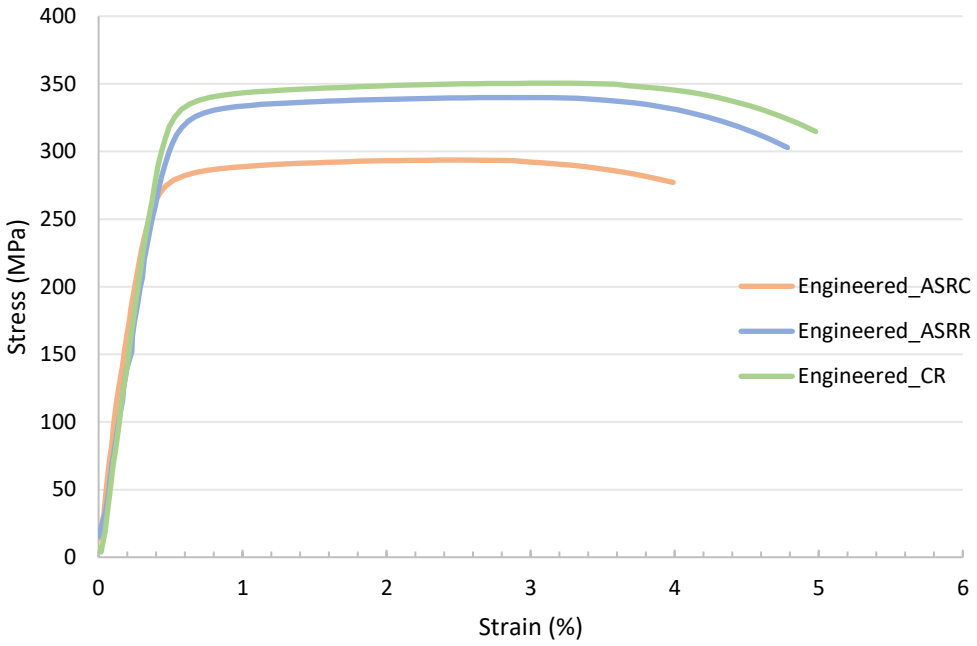

Figure 46: Example of Engineering and True stress-strain curves (from CR).

The figure shows an example of the curves that are analysed. The same analysis was made for each trial; however, the obtained data is contained in the tables 9 and 10, therefore not needing the curves representation. Considering the information gathered until this point, there are a few things than can be assumed and others that can be questioned.

The general overview is that the after rolling, SHT1 shows less improvement in the hardness of the alloy than the SHT2.Even though the mechanical properties obtained by the tensile tests revealed that it increased, there is not enough information to establish a concrete conclusion. Bearing in mind all batches of tests, it is obvious that the elongation at break reduced significantly regarding the initial material.

Several circumstances in the first tests justify the lack of precision in the data.

The two main conclusions of this step are:

i) for future tests, the ASR (15/5) revealed to be valueless since the rolling mill does not work well under those velocities;

ii) ii) the relation between the HV and the tensile strength of the material proves to be correlated since there is a match in the magnitude of the values (even though it is a rough one).

Elongation decreased drastically when compared to the T6 temper. A lot of strain was induced into the samples. For now, the material's lack of deformability is an indicator that it should be enhanced. The SHT1 was the chosen one to continue the rest of the work because requires a shorter time for heat treatment then SHT2, which represents less energy consumed. The aim of this work is to find a cheaper solution to the expensive T6 temper, so the SHT1 and natural aging combination present the best cost-effective solution. SHT2 was four times more time consuming for a similar temperature, therefore, it is not considered from this point on.

4.2. Step 2 – Reduction per pass

Two sets of reduction per pass (rpp) were considered in the second set of tests.
As mentioned in the previous step, only SHT1 samples were submitted to the following rolling sequences (figure 47).

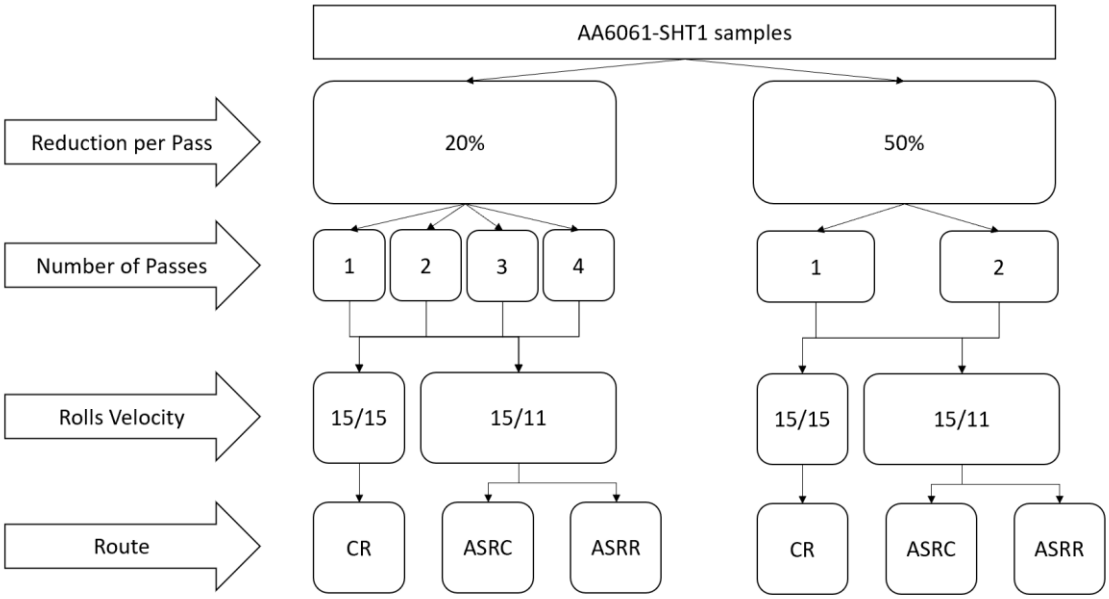

Figure 47: Schematic of carried out processes (step 2).

This time, the effects of each rpp (20% and 50%) are studied. Tensile tests were made for each sample. Uniaxial tensile tests were made to verify the mechanical properties of all rolling sequences. Since these tests are more complete, hardness tests were not used for this step (table 12 and 13).

Table 12: Mechanical properties obtained for rolling with 20% reduction per pass.

No. Passes	20%		Yield Stress (MPa)	Ultimate Strength (MPa)	Elongation at Break (%)
1	CR	1	206.29	230.48	10.07
		2	210.64	233.66	11.30
		3	201.75	227.73	12.55
	ASR	1	229.06	251.04	10.06
		2	236.01	254.91	9.09
		3	190.08	201.18	7.31
2	CR	1	223.80	230.75	5.87
		2	228.70	227.69	5.95
		3	212.40	218.47	3.95
	ASRC	1	256.34	267.24	5.86
		2	251.44	264.35	5.10
		3	255.18	268.45	6.08
	ASRR	1	218.64	221.52	3.99
		2	222.87	228.96	5.18
		3	224.55	231.35	5.44
3	CR	1	278.16	288.65	5.77
		2	278.00	288.37	5.92
		3	280.15	291.50	6.01
	ASRC	1	267.53	276.63	4.77
		2	265.65	275.99	4.93
		3	263.00	273.11	5.09
	ASRR	1	274.42	284.92	5.11
		2	267.00	278.58	4.30
		3	272.42	281.06	4.87
4	CR	1	-	-	-
		2	255.03	255.66	4.14
		3	255.07	258.06	4.08
	ASRC	1	308.54	317.47	4.15
		2	306.72	318.06	4.27
		3	307.30	318.38	4.45
	ASRR	1	266.58	270.50	2.65
		2	264.39	269.08	3.97
		3	267.13	269.67	3.74

For 20% reduction rate, results vary in different ways. There is a slight increase in the values of strength with each pass of rolling, whether it is Yield or Ultimate Strength. A decrease in elongation follows it from pass 1 to 4. The CR and ASRR samples register an intermediate increase in elongation in the third pass. The overall analysis was made by comparing the mean values of strength and elongation for each rolling sequence. The curves are as presented below (figure 48).

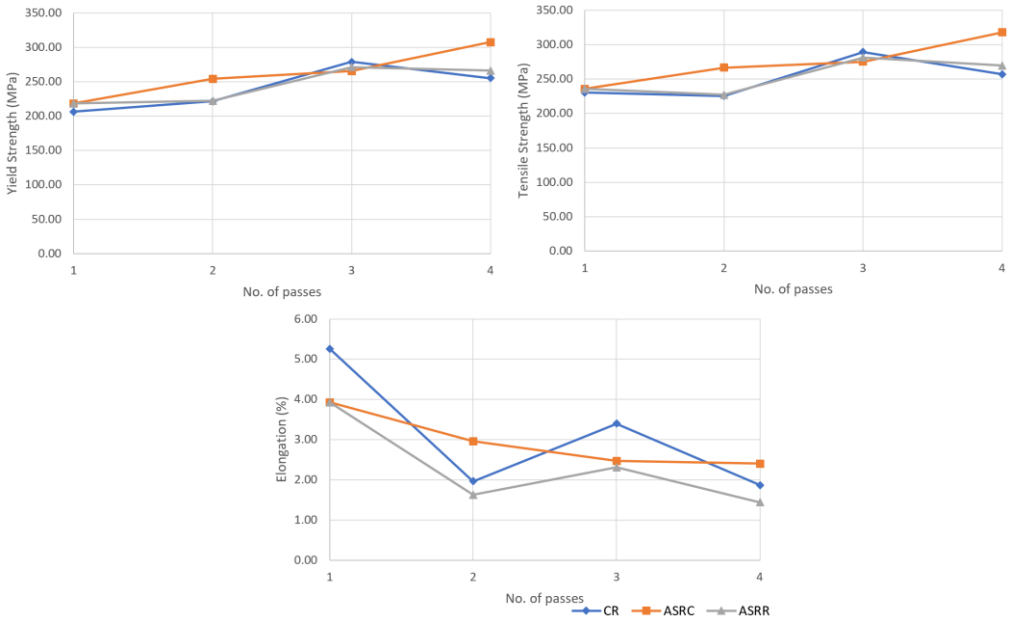

Figure 48: Effects of the number of passes in the mechanical properties of samples.

While the ASRC shows a continuous rising in strength from one to four passes, the ASRR shows intermittent increases of elongation and decreases of strength. For example, the first and third pass of ASRR register comparatively high values of tensile strength, unlike the second and fourth, in which this same tensile strength stalls. The inversion of the rolling direction is supposed to be the main cause of this phenomena. The shear strain induced in the samples cancel themselves out with the next pass.

The trend of conventional rolling is to rise in each pass, however, the pic values for CR seem to appear upon the third reduction. Notwithstanding, the difference between the values registered for three to four passes is near 10 MPa.

Table 13: Mechanical properties obtained for rolling with 50% reduction per pass.

No. Passes	50%		Yield Stress (MPa)	Tensile Strength (MPa)	Elongation at break (%)
1	CR	1	260.82	270.46	5.90
		2	260.30	272.25	5.96
		3	256.44	266.60	5.26
	ASR	1	-	-	-
		2	-	-	-
		3	-	-	-
2	CR	1	296.98	307.14	4.91
		2	294.28	304.18	5.25
		3	293.81	302.06	5.15
	ASRC	1	264.50	269.09	2.85
		2	267.10	268.93	2.47
		3	265.84	266.71	2.37
	ASRR	1	261.90	266.22	3.06
		2	255.70	261.33	3.43
		3	254.45	260.76	3.53

The results of one pass of ASR, with a 50% reduction rate, do not appear in the table. The samples with this sequence were damaged and because of that, it was impossible to obtain data.
The values of strength for this reduction rate are bigger in the CR configuration, not in the ASR, as in the 20% pass rate.
One of the main aspects that contrast between the 20% to 50% reduction rate is the elongation values. In general, elongation in 50% rpp values is smaller than the 20% rpp. The more percentage of reduction one applies, the more strain the material will suffer, accumulating more dislocations and making it stiffer and less workable. The rest of the data from the 50% passages is very similar, ranging 250 to 270 MPa. The obtained values comprehend comparative limitations due to different rpp's. The results obtained throughout this step start to compose the behaviour of the worked aluminium when subjected to rolling processes.
To support the results obtained, a new batch of tests was conducted in the following step.

4.3. Step 3 - Effects of material heat treatment

In this step, 2 and 4 passes for 50% rpp and 20 % rpp were studied. Not only the cold working was carried out during this step, but also an annealing heat treatment (AHT) was applied after rolling.
The aim behind the AHT after rolling was to enhance the low values of formability registered in previous measurements. It is important not to overdo the heating period as it may affect the strength properties enhanced before (figure 49).

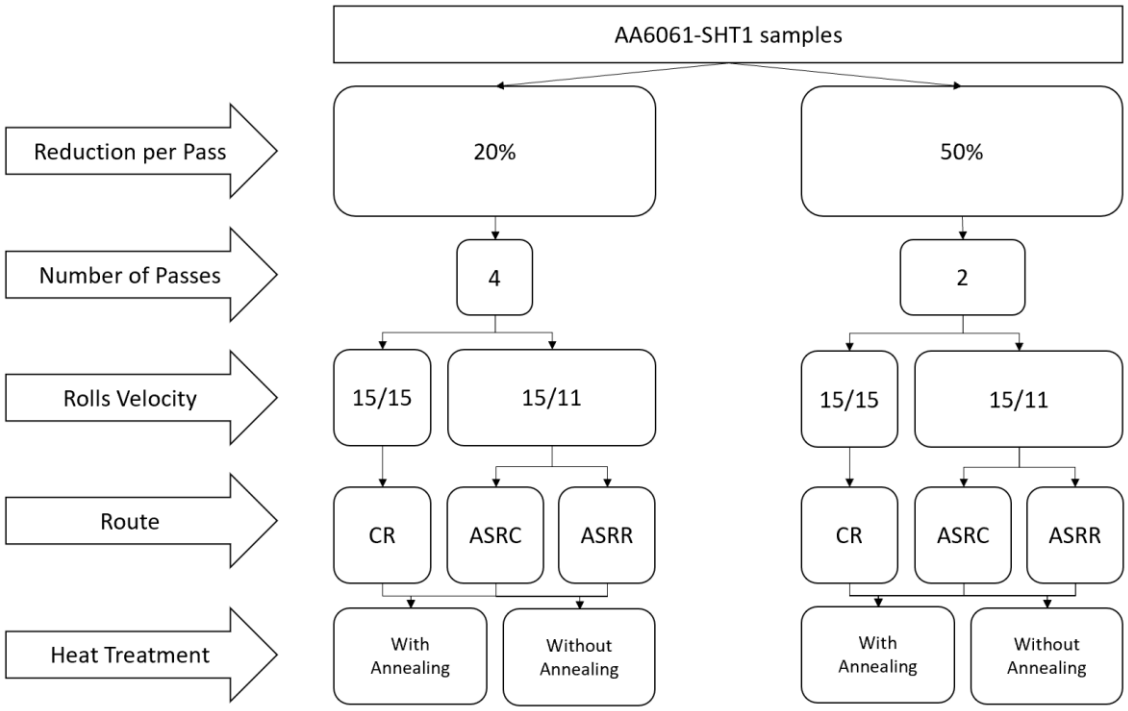

Figure 49: Schematic of carried out processes (step 3).

The AHT temperature used was 200ºC, for the duration of 60 minutes. In this case, the samples were introduced in the furnace after it reached the desired temperature. The cooling of the samples was done by air at room temperature (circa 25ºC). The annealing heat treatment diagram is shown in (figure 50).

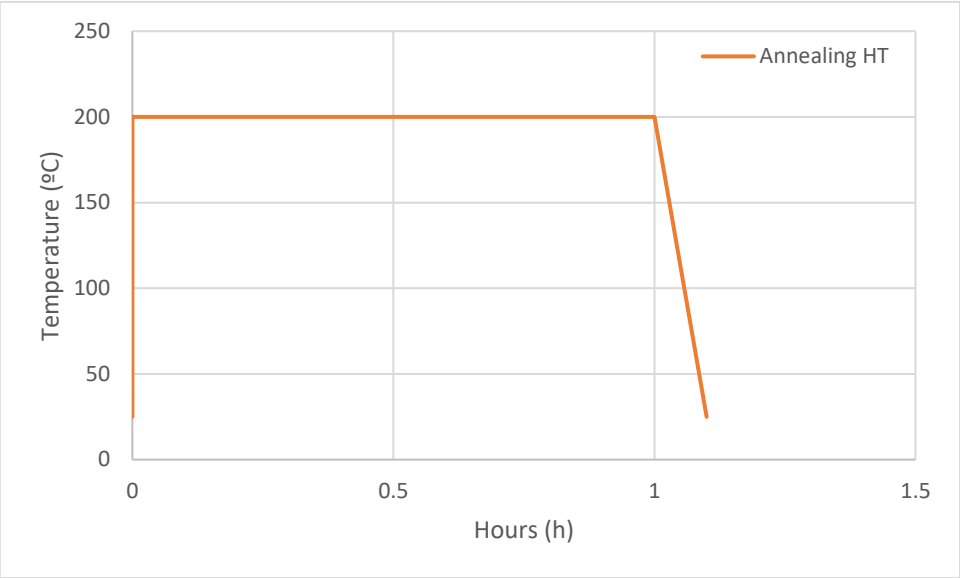

Figure 50: Annealing Heat Treatment applied after rolling.

The work related to this step is divided in 4 phases:

i) Production and verification of the SHT1 in the material;
ii) Processing de material by CR and ASR;
iii) Annealing after cold rolling;
iv) EBSD analysis.

To avoid any problems during the SHT, the samples were divided into smaller groups in order to ensure the homogeneity of the heating inside of furnace for each sample. To verify if that the initial properties were the same for all the samples, the hardness of this material was measured. The mean value obtained from this measurement was 80 HV with maximum deviations of 4HV.
As a starting point, three samples of the solubilized aluminium were tested (figure 51).

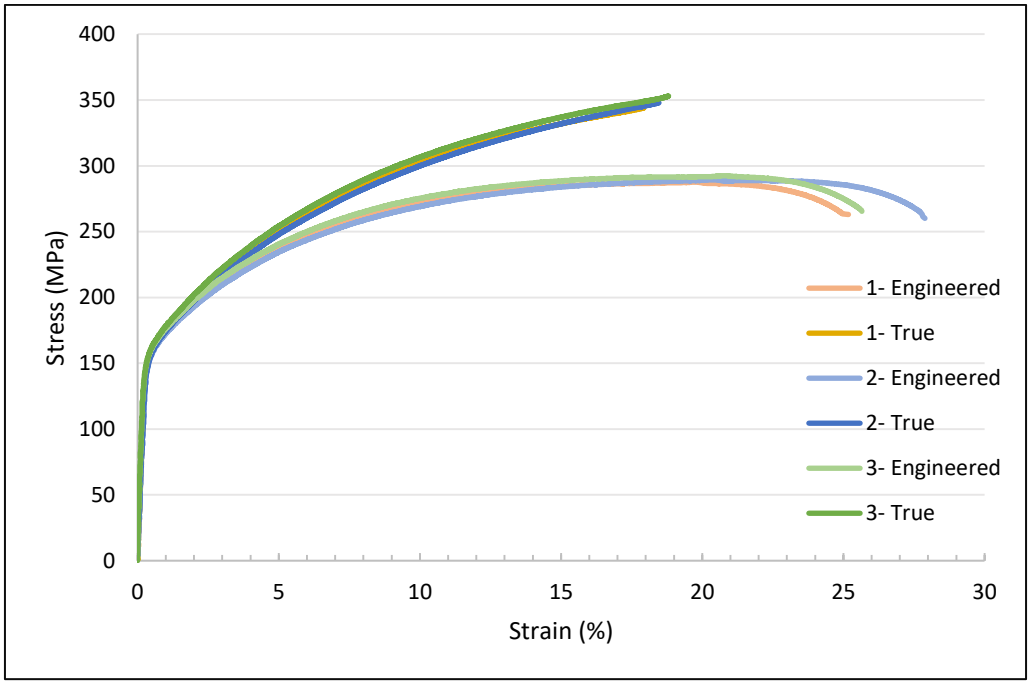

Figure 51: True stress-strain curves for samples after SHT1.

A Yield Strength of 158.12 MPa, Ultimate Tensile Strength of 289.86 MPa and Elongation at break of 26.24% was obtained from the measured stress-strain curves.
The most evidenced property of the solubilized aluminium is its high formability. Differently, the Yield Strength is relatively low, when compared to the T6 or even other rolled samples tested before.
The samples were then analysed by EBSD (figure 52).

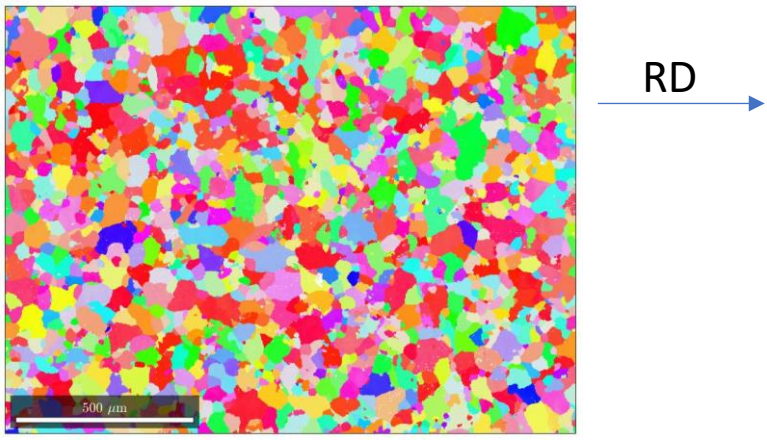

Figure 52: SHT1 texture.

Well-defined grains are observed with an average size about 50 µm. Regarding their orientations, the pole figures and the ODF's is presented in figure 53.

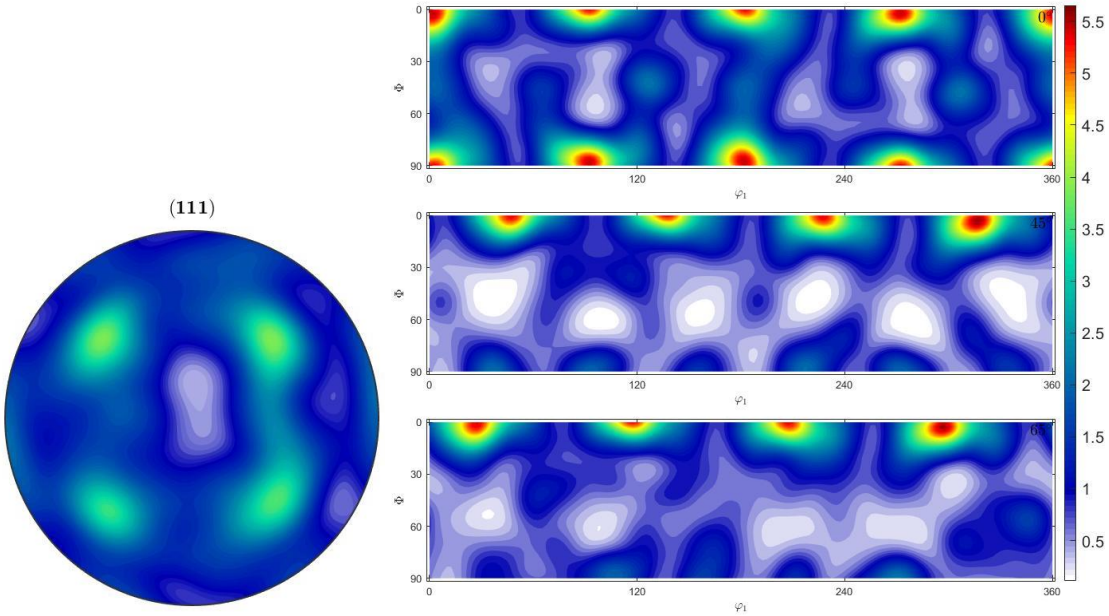

Figure 53: PF and ODF representation of SHT1 texture components.

The only texture component strongly evidenced was Cube {100}<001>, which is commonly found in recrystallized aluminium alloys. This proves the aluminium samples undergone recrystallization as intended.

The different combinations of materials resulted from the mix of SHT, rolling and AHT, were subdivided into NAS (not annealed samples) and AS (annealed samples). For all these configurations, uniaxial tensile tests were done, and the respective stress-strain curves were obtained (figure 54 to 57).

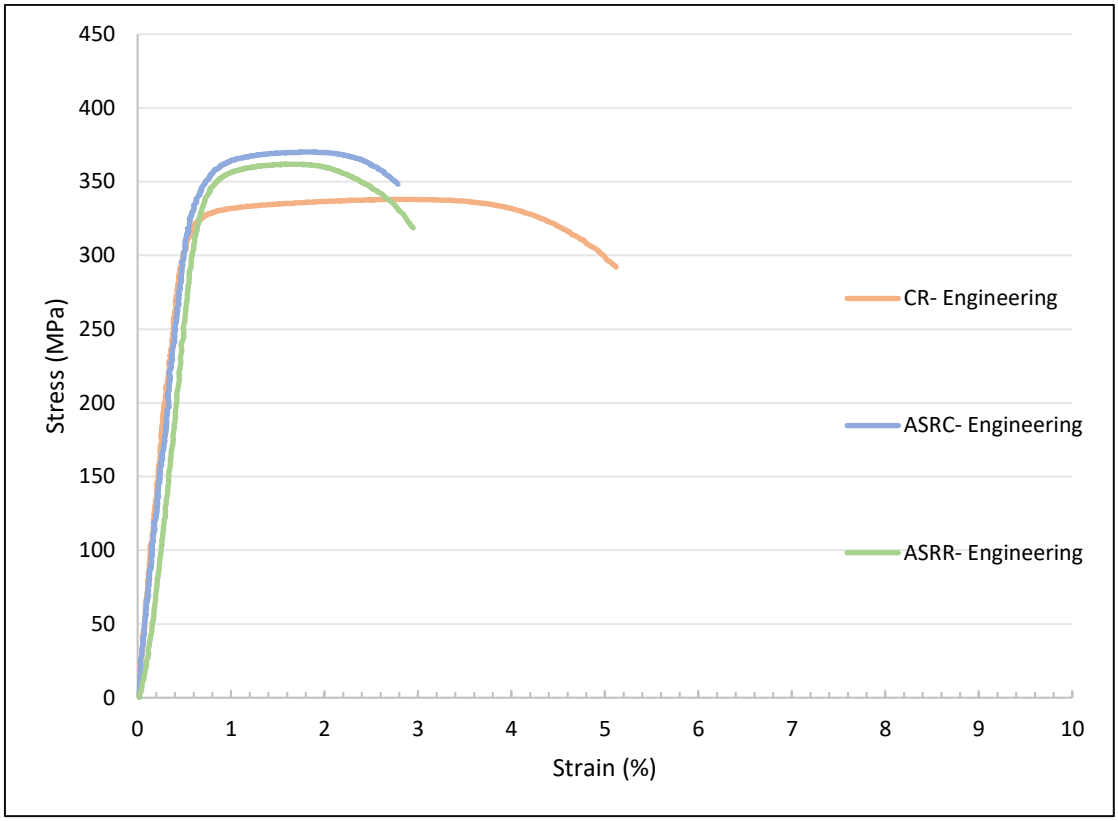

Figure 54: 20% rpp NAS stress-strain curves.

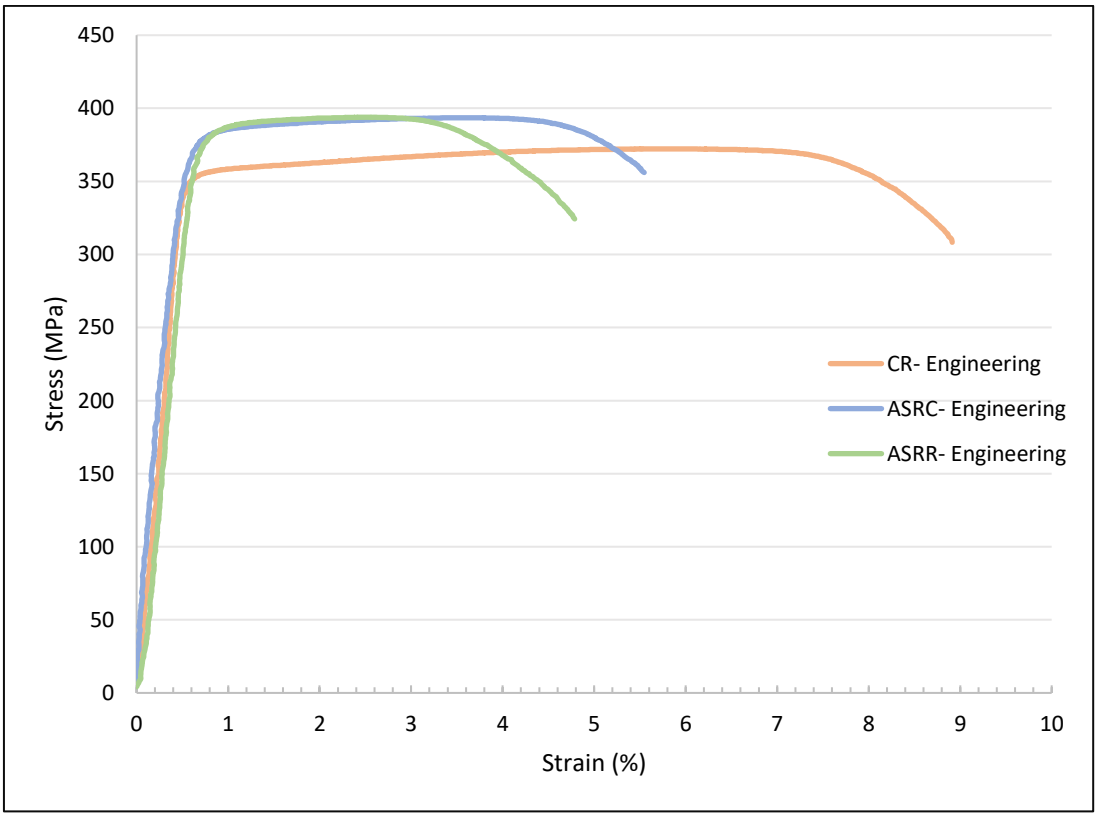

Figure 55: 20% reduction rate AS stress-strain curves.

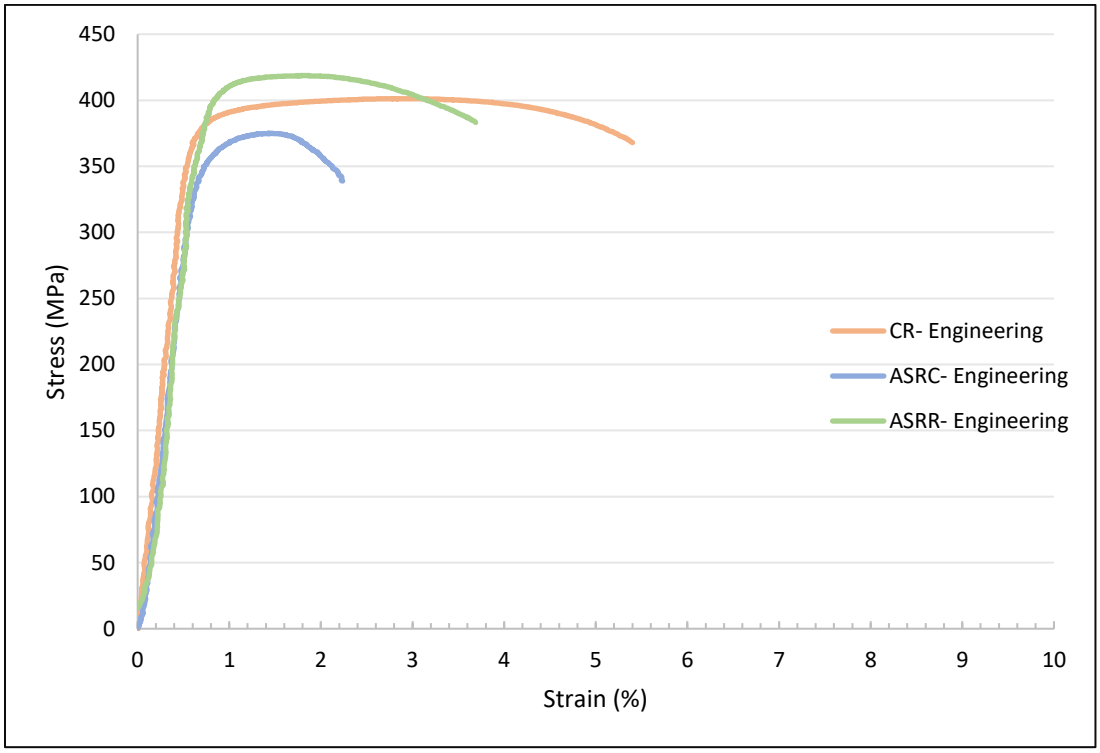

Figure 56: 50% reduction rate NAS stress-strain curves.

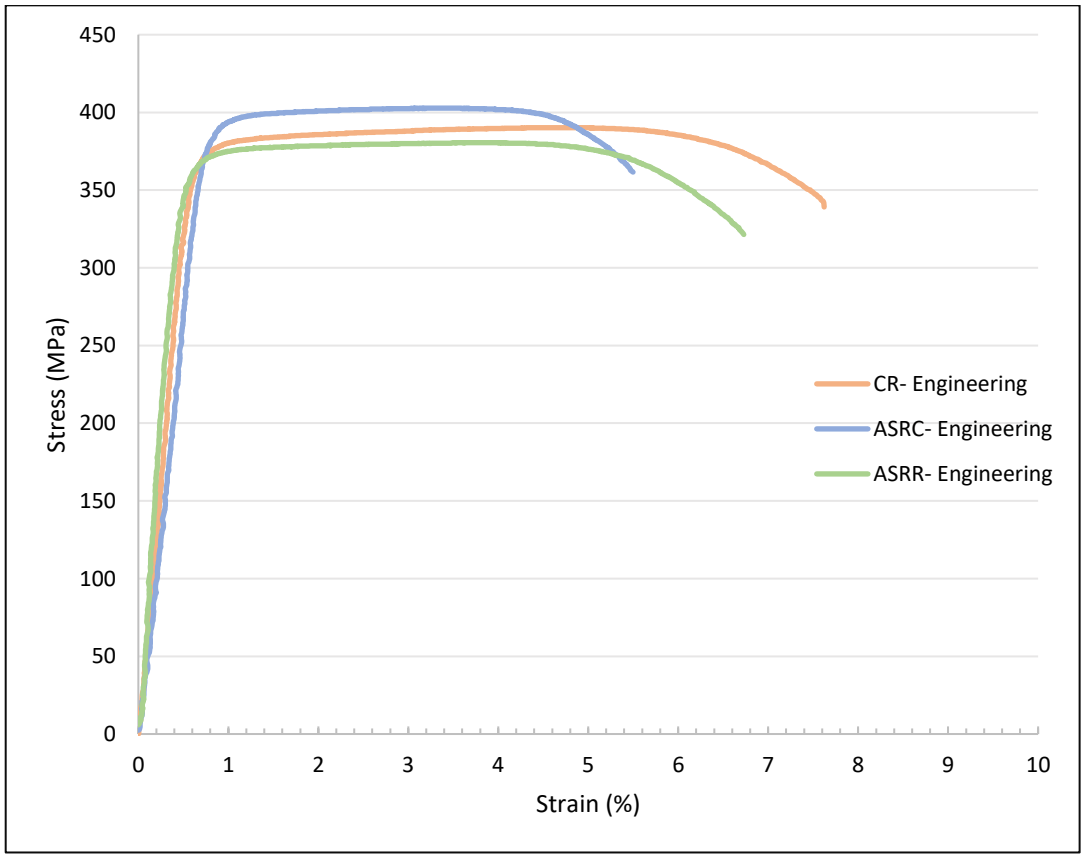

Figure 57: 50% reduction rate AS stress-strain curves.

The stress-strain curves of the tested samples allowed the evaluation of its mechanical properties (figures 58 and 59).

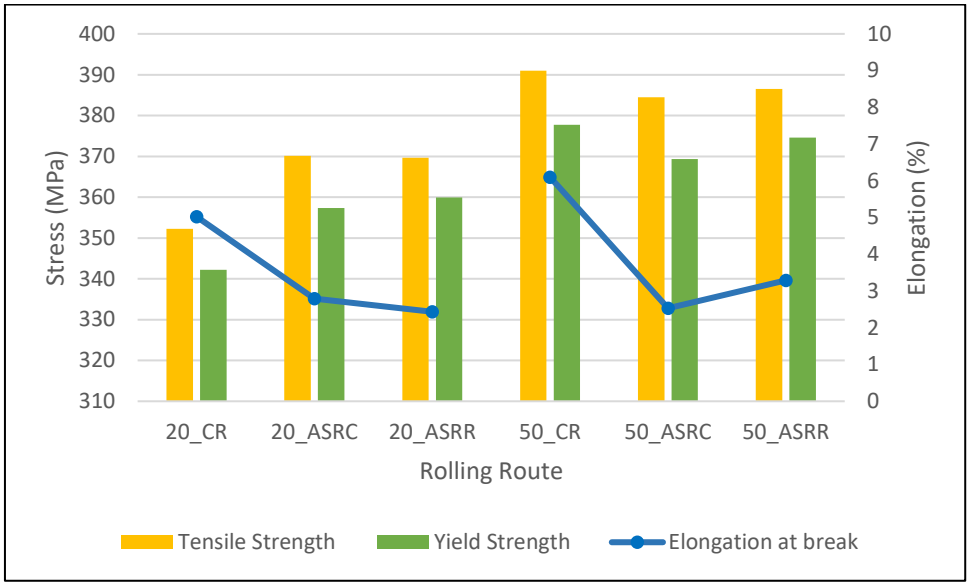

Figure 58: Mechanical properties of NAS.

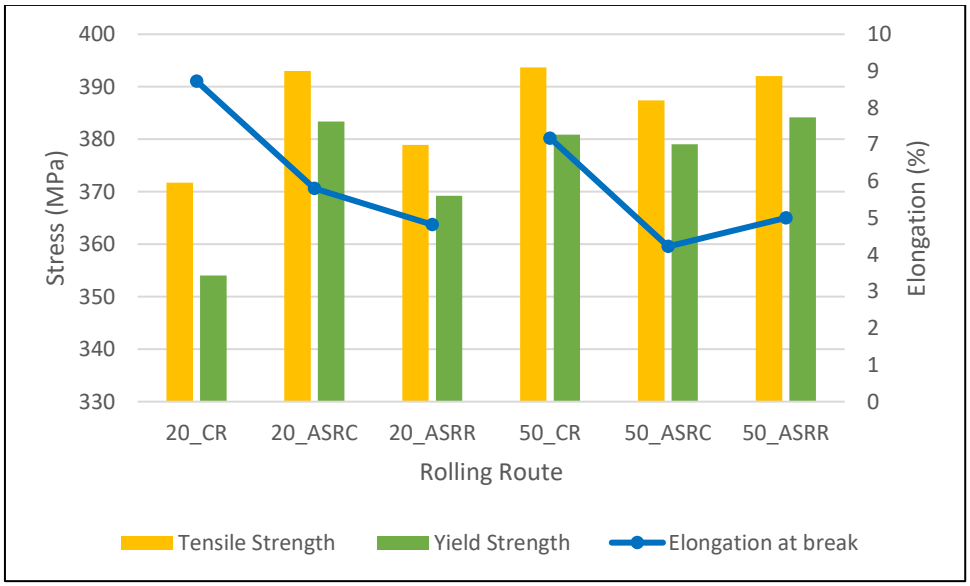

Figure 59: Mechanical properties of AS.

There are clear points for both NAS and AS. CR presents higher values of elongation at the breaking point, however, the strength of the material is less than those samples subjected to ASR, when considered the same reduction rate.

For NAS the strength of the 50% reduction rate is higher than the same tested routes for 20%. Following this trend, a simultaneous decrease in the elongation of the samples is worth mentioning. The mechanical properties of the AS do not illustrate a clear distinction as the NAS. It is evident

though, that the combination that presents the worst values of strength is the conventional rolled samples at 20% reduction rate, however, they also show the best elongation values. In conventional rolled at 50% reduction rate samples, the elongation continues to be the higher than the values registered for asymmetrical rolling, but the values of strength are oddly high. These values are in opposition with previous results.
Between ASRC and ASRR samples, the values of strength and elongation are very similar in both AS and NAS. The readings of the obtained data show that from ASRC to ASRR there is a decrease in elongation at 20% rpp and an increase at 50% rpp. A decrease of strength is also noted for 20% and an increase for 50% reduction rate. Even though this comparison is evidenced in the figures 53 to 58, the differences in values are so small that it would be inaccurate to stablish an absolute comparison between the two ASR routes.
Even after the annealing heat treatment, the strength of the material gained via strain hardening, was not affected, allowing a slight increase in formability without losing its gains.
When applied an ASR process with 50% reduction rate, the amount of deformation in the samples was massive, what lead to the bending (figure 60).

Figure 60: Bending of samples due to ASR with 50% reduction rate, 1 pass (left) and 2 passes (right).

The excessive strain applied, and the heat generated from it could interfere with the aluminium crystalline structure, affecting its mechanical properties.
To further characterize the microstructure evolution of AS, the EBSD analyses was used (figures 61 and 62).

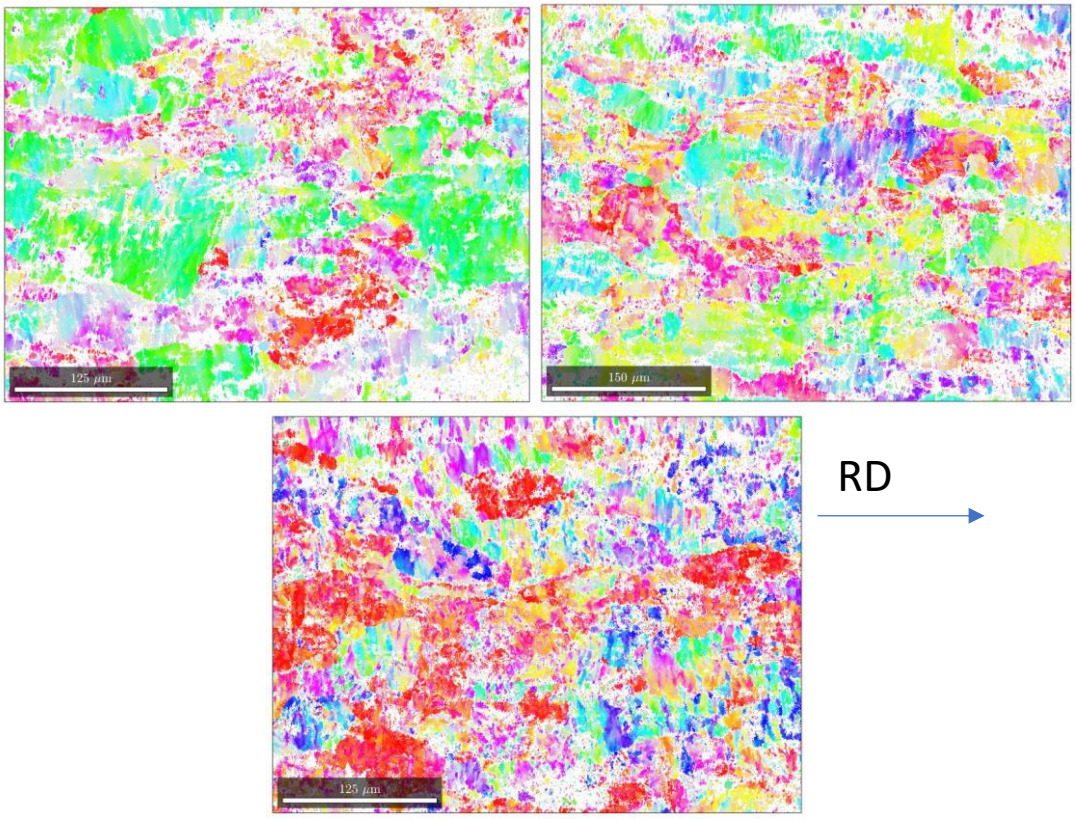

Figure 61: EBSD images of a) 20_CR; b) 20_ASRC; c) 20_ASRR after 4th step

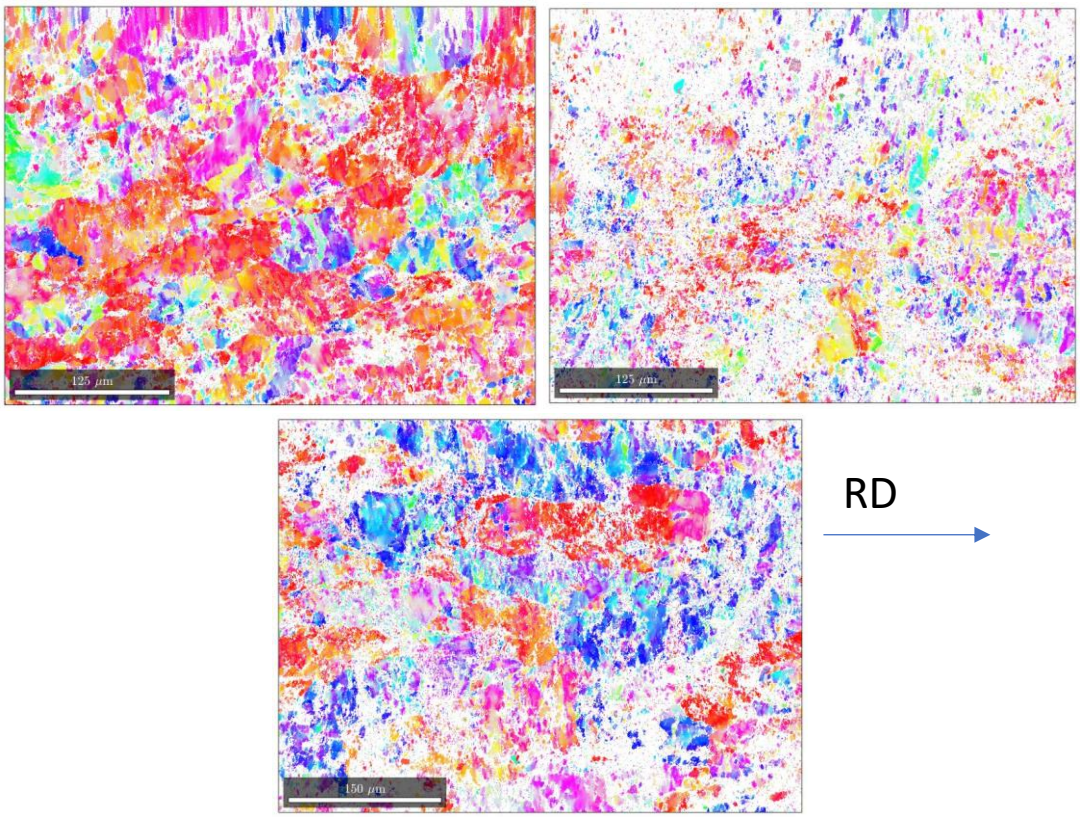

Figure 62: EBSD images of a) 50_CR; b) 50_ASRC; c) 50_ASRR after 2nd step

The grain size evolution revealed to be difficult to obtain due to the ambiguity of grain boundary identification. As a general trend, it seems that the reduction of grain size was promoted by rolling. This affirmation is based on the "information map" provided by the software "Espirit 1.9" available with the EBSD analysis, which only grains larger than 100 pixels (on the produced image) are considered by the used software.
ODF's and Pole Figures for the different sample configurations were analyzed (figure 63).

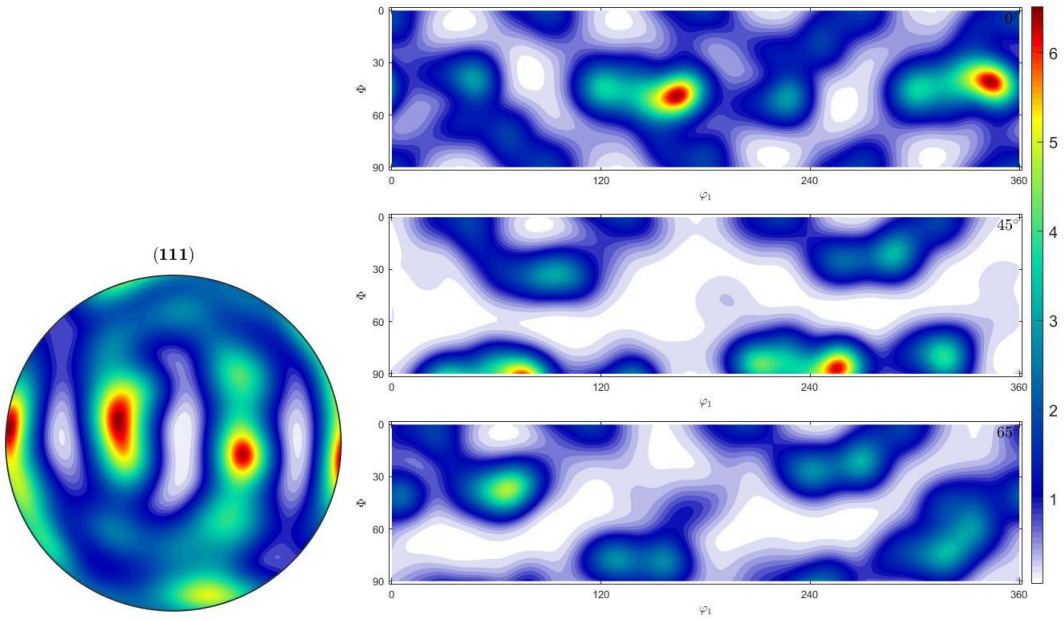

Figure 63: PF (left) and ODF (right) of annealed sample 20_CR.

The two representations of the texture components were necessary to identify the selected samples. It is not always clear the agglomerate of grain orientation density.
The typical FCC texture components found in the sample were: Brass {011}<211> and S {123}<634>. These deformation components are mostly evidenced in $\varphi_2 = 45°/\ \varphi_1 = 60°\ /\phi = 90°$ for Brass and $\varphi_2 = 45°/\ \varphi_1 = 60°\ /\phi = 90°$ for S. Brass and S are characteristic of conventional rolled aluminium alloys. Cube {100}<001> and P {011}<112> were not found in this sample.
The same process was carried on for the different samples, PFs and ODFs were studied (figures 64 to 68).

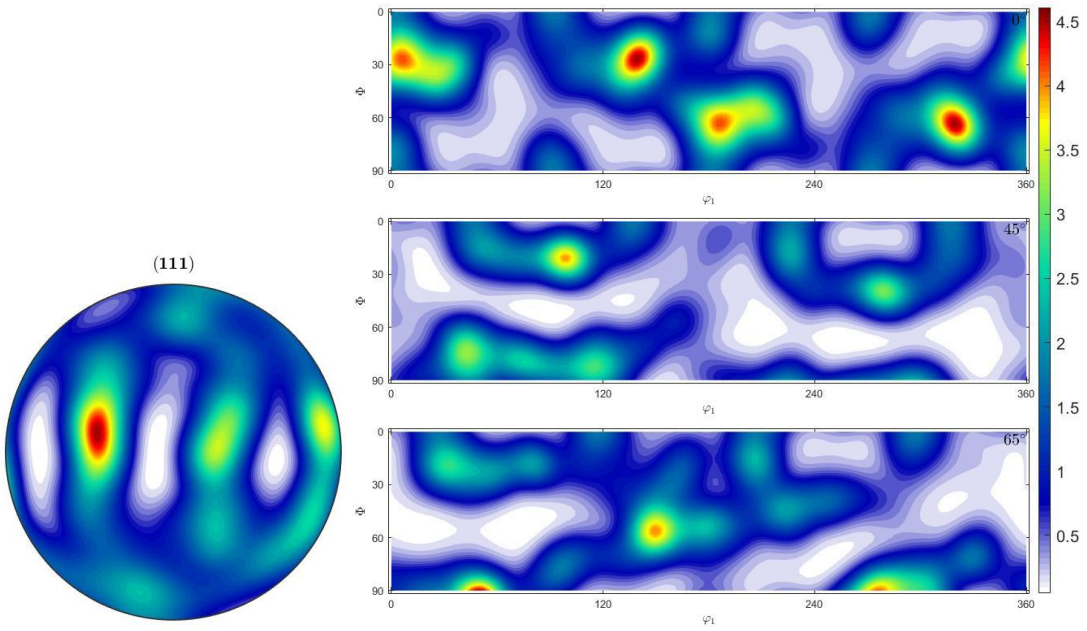

Figure 64: 20_ASRC PF and ODF.

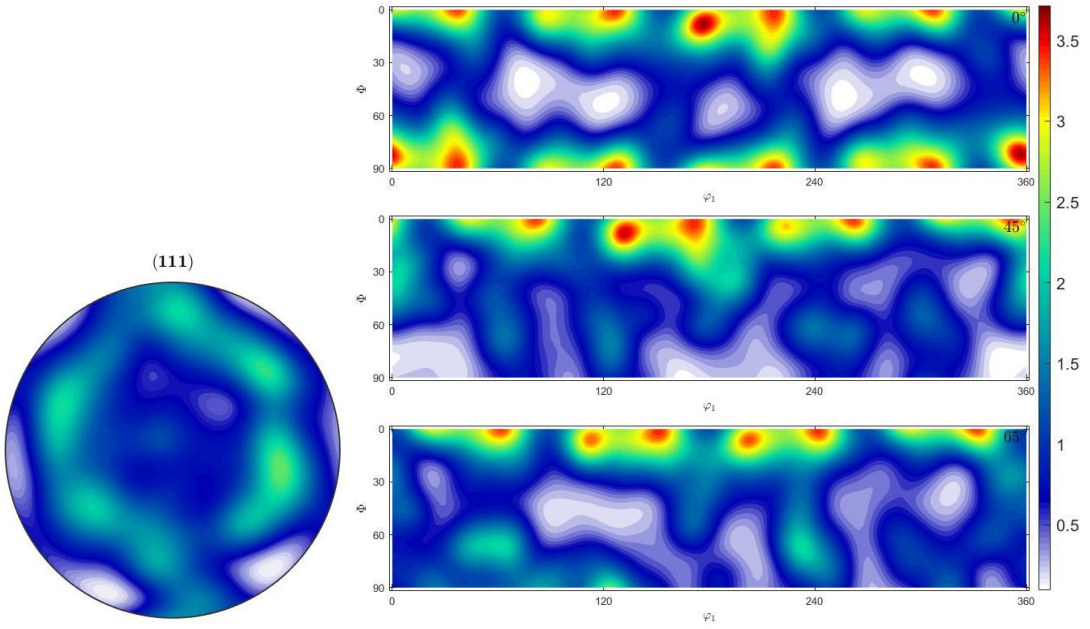

Figure 65: 20_ASRR PF and ODF.

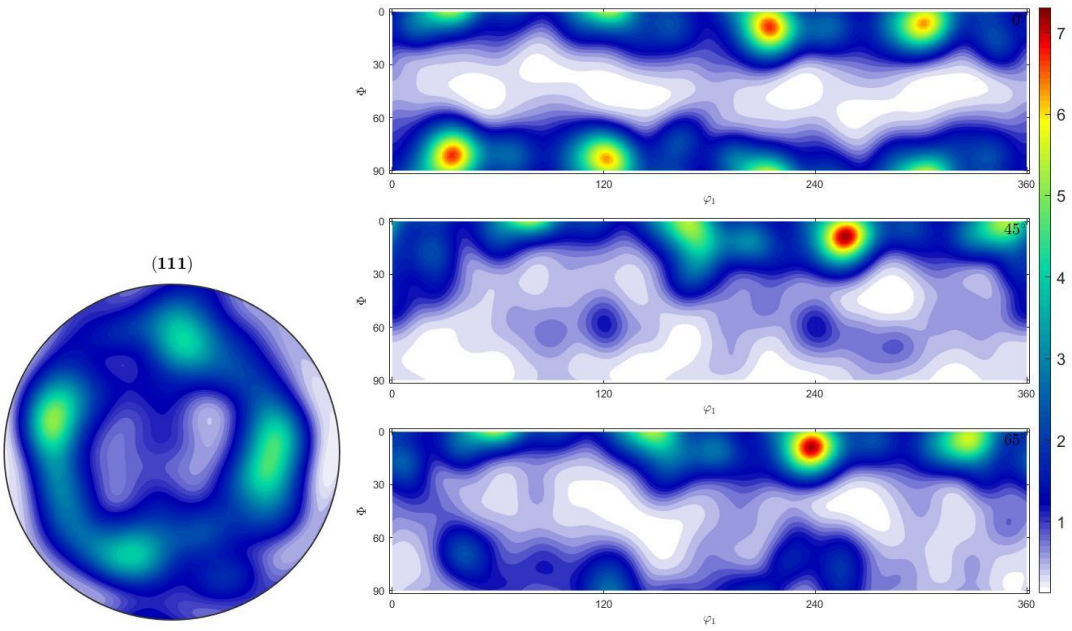

Figure 66: 50_CR PF and ODF.

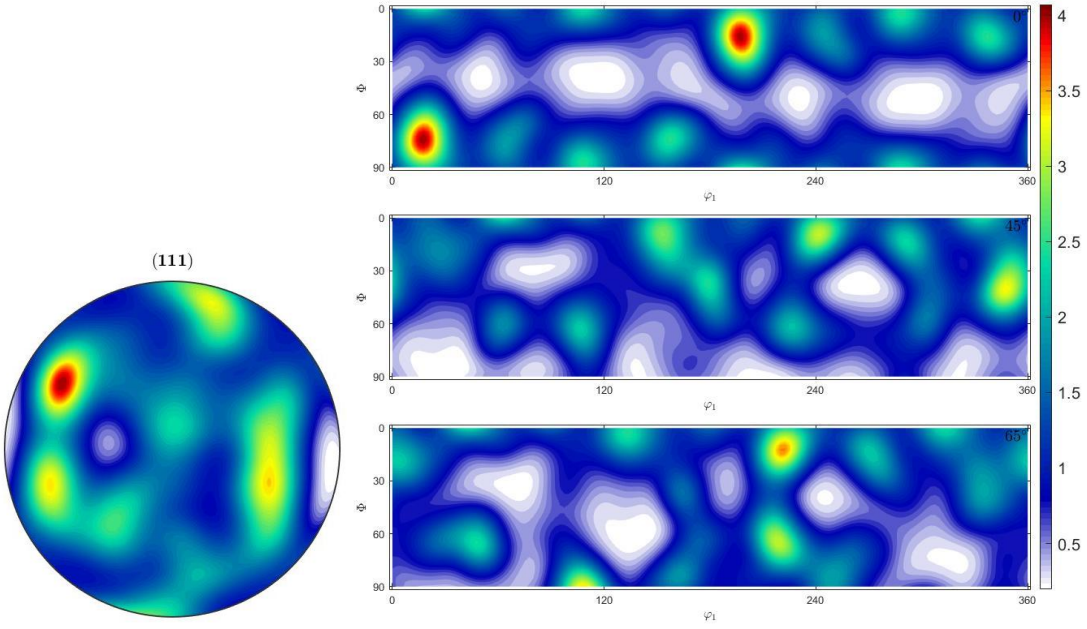

Figure 67: 50_ASRC PF and ODF.

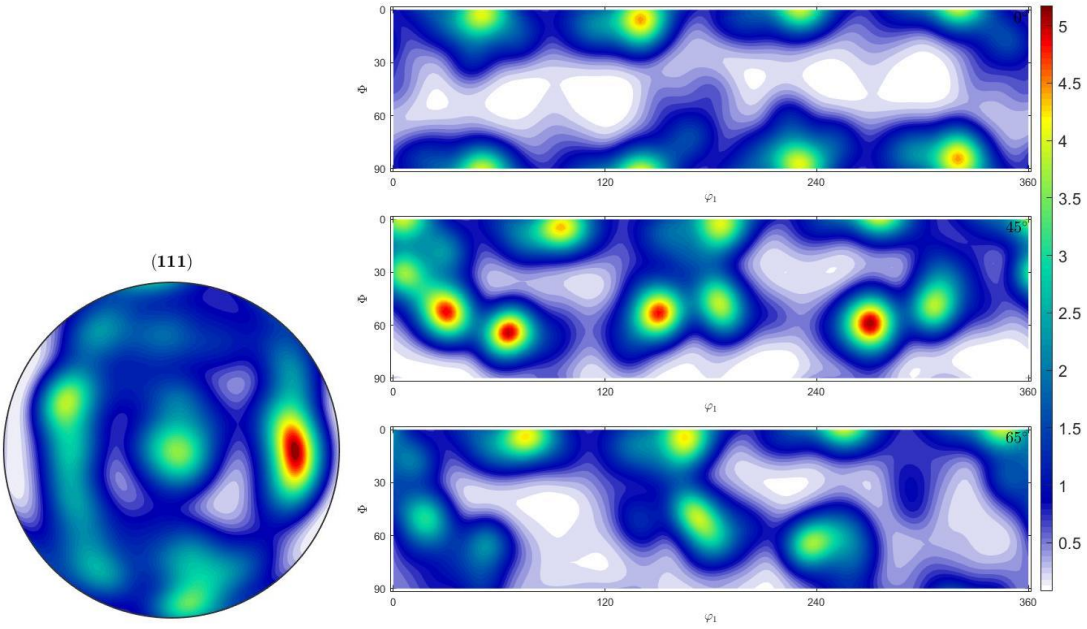

Figure 68: 50_ASRR PF and ODF.

The interpretation of the previous figures led to the following results (table 14).

Table 14: Texture components of AS. (s)-strong presence, (m)-medium presence.

AS	Deformation Comp.	Recrystallization Comp.
20_CR	β fibre (Brass (s), S (m), Copper (m))	Cube (m), Goss(m)
20_ASRC	Copper (s)	RCrd1 (s), Cube(m), P (m)
20_ASRR	H (s)	Cube (m)
50_CR	H (m), F(m)	-
50_ASRC	H(s), F(m), Brass(m)	-
50_ASRR	H (s), F (s)	-

The shear components H and F are observed in the ASR samples. It is surprising the presence of these two components on the CR sample since no shear was supposed to be promoted during symmetric rolling. An explanation for their presence can be the existence of different friction coefficients between the rolls and the two surfaces of the sheet that can produce an undesired shear deformation during rolling. In the samples produces with 20 rpp, are present some recrystallization components. It is not possible to confirm that these components are retained during rolling or are created during annealing. This can be verified in the future by EBSD analysis after each pass of rolling.

(Page intentionally left blank)

5. Conclusion

The type of rolling (CR, ASRC and ASRR) and reduction per pass were the main strength improvement agents of the studied aluminium alloy. These values of strength surpassed the ones that AA6061-T6 registers. However, the deformability of the alloy after rolling was considerably low. Ensuing annealing heat treatments slightly improved this mechanical property without affecting the increased values of strength.

The tests lead to believe that CR, compared to ASR, registers a smaller increase in strength. Linked with this, the formability of the aluminium is less affected, resulting in the most workable / high strength option. The observation of the texture through EBSD does not enable concrete conclusions regarding the grain size due to the difficulty to visualize the frontiers of grains. However, it is believed that some reduction of grain size occurred.

Improved AA6061, enhanced by strain hardening, emerge as a promising option to the already used AA061-T6. Overall, the results show that the yield strength increased a minimum of 40% when submitted to rolling and annealing processes and a maximum of 56% (for AS referred in chapter 4). Following the increasing strength, the samples register a reduction in formability by more than half. ASR samples had values ranging from 4.2% to 8.7% of elongation at break.

AA6061 has been used for a long time in the aerospace industry. This study defends that, with more economic metal forming processes, it is possible to produce high-quality materials that merge with the plans of the aerospace and aeronautical industry.

5.1. Future work suggestions

Founded on the results gathered in the present work, a few suggestions for future works are listed:

- A more in-depth analysis of the texture, correlating it to the obtained mechanical properties (grain size, orientation and misorienations) of the tested routes.
- Enhancing the formability of post-rolled samples using new configurations of annealing heat treatments.
- Explore new rolling parameters for ASR such as thickness reduction and speed ratios.

(Page intentionally left blank)

References

AMAG Rolling GmbH. (2012). AMAG ADVANCED AA6061 ALLOY FOR AEROSPACE APPLICATIONS. *AluReport*, 12–13.

Aruga, Y., Kozuka, M., Takaki, Y., & Sato, T. (2015). Formation and reversion of clusters during natural aging and subsequent artificial aging in an Al-Mg-Si alloy. *Materials Science and Engineering A*, *631*, 86–96. https://doi.org/10.1016/j.msea.2015.02.035

Avitzur, B. (1983). *Handbook of metal-forming processes: A Wiley-Interscience publication*. John Wiley and Sons.

Azimi-Roeen, G., Kashani-Bozorg, S. F., Nosko, M., & Orovcik, L. (2018). EBSD investigation of Al/(Al 13 Fe 4 +Al 2 O 3) nanocomposites fabricated by mechanical milling and friction stir processing. *Journal of Microscopy*, *270*(1), 3–16. https://doi.org/10.1111/jmi.12642

Bahrami, A., Miroux, A., & Sietsma, J. (2012). An age-hardening model for Al-Mg-Si alloys considering needle-shaped precipitates. *Metallurgical and Materials Transactions A: Physical Metallurgy and Materials Science*, *43*(11), 4445–4453. https://doi.org/10.1007/s11661-012-1211-8

Berneder, J., Prillhofer, R., Schulz, P., & Melzer, C. (2017). Characterization of Pre-Aged AA6061-T6 Sheet Material for Aerospace Applications. *ICAA13 Pittsburgh*, 1797–1802. https://doi.org/10.1007/978-3-319-48761-8_269

D. Callister Jr., W., & G. Rethwisch, D. (2011). *Materials Science and Engineering: An Introduction* (8th ed.). Hoboken: John Wiley & Sons, Inc.

Koch, T., Bierögel, C., & Seidler, S. (2014). Conventional Hardness Values - Application. In *Polymer Solids and Polymer Melts–Mechanical and Thermomechanical Properties of Polymers* (pp. 428–430). Springer Berlin Heidelberg. https://doi.org/10.1007/978-3-642-55166-6_71

MatWeb, L. (2019). ASM Material Data Sheet. Retrieved December 3, 2019, from http://asm.matweb.com/search/SpecificMaterial.asp?bassnum=MA6061T6

Mirzakhani, B., & Mansourinejad, M. (2011). Tensile properties of AA6061 in different designated precipitation hardening and cold working. *Procedia Engineering*, *10*, 136–140. https://doi.org/10.1016/j.proeng.2011.04.025

Polat, A., Avsar, M., & Ozturk, F. (2015). Effects of the artificial-aging temperature and time on the mechanical properties and springback behavior of AA6061. *Materiali in Tehnologije*, *49*(4), 487–493. https://doi.org/10.17222/mit.2013.154

Schmid, F., Uggowitzer, P. J., Schäublin, R., Werinos, M., Ebner, T., & Pogatscher, S. (2019). Effect of thermal treatments on Sn-alloyed Al-Mg-Si alloys. *Materials*, *12*(11), 1801. https://doi.org/10.3390/ma12111801

Shore, D., Kestens, L. A. I., Sidor, J., Van Houtte, P., & Van Bael, A. (2018). Process parameter influence on texture heterogeneity in asymmetric rolling of aluminium sheet alloys. *International Journal of Material Forming*, *11*(2), 297–309. https://doi.org/10.1007/s12289-016-1330-7

Simões, F. J. P. (2008). Tese Doutoramento - Estudo da laminagem assimétrica na liga de alumínio 1050. *UA*.

Staley, J. T., & Lege, D. J. (1993). Advances in aluminum alloy products for structural applications in transportation. *Journal De Physique*, *3*(7 pt 1), 179–190.

Starke, E. A., & Staley, J. T. (1996). Application of modern aluminum alloys to aircraft. *Progress in Aerospace Sciences*, *32*(2–3), 131–172. https://doi.org/10.1016/0376-0421(95)00004-6

Tamimi, S. (2013). Asymmetric rolling of 5182 aluminium alloy and interstitial free steel sheets. *UA*. Tese de Doutoramento

Wulff, J., Moffatt, W. G., Pearsall, G. W., Brophy, J. H., Rose, R. M., Hayden, H. W., … Klerer, J. (1967). The Structure and Properties of Materials. *Journal of The Electrochemical Society*, *114*(9), 243C. https://doi.org/10.1149/1.2426767

Xu, Z., Liu, X., Chen, R., & Shan, D. (2019). Optimal thermal process parameters of hot stamping AA 6061. In *IOP Conference Series: Materials Science and Engineering* (Vol. 612). https://doi.org/10.1088/1757-899X/612/3/032024

Zhang, S., Li, X., Chen, C., Jeong, H., & Xu, G. (2019). Characterization of Aging Treated 6061 Aluminum Alloy Using Nonlinear Rayleigh Wave. *Journal of Nondestructive Evaluation*, *38*(4), 88. https://doi.org/10.1007/s10921-019-0630-5

Zhang, X., Yu, Y., Liu, B., Zhao, Y., Ren, J., Yan, Y., … Chen, J. (2020). Microstructure characteristics and tensile properties of multilayer Al-6061/Ti-TA1 sheets fabricated by accumulative roll bonding. *Journal of Materials Processing Technology*, *275*. https://doi.org/10.1016/j.jmatprotec.2019.116378

Zhou, D., Du, W., Wen, X., Qiao, J., Liang, W., & Yang, F. (2018). Local Deformation and Texture of Cold-Rolled AA6061 Aluminum Alloy. *Materials*, *11*(10), 1866. https://doi.org/10.3390/ma11101866